

Fabrication of micro separation column for miniaturized gas chromatography system

Greeshma P. M.

A Thesis Submitted to
Indian Institute of Technology Hyderabad
In Partial Fulfillment of the Requirements for
The Degree of Master of Technology



Department of Electrical Engineering

July 2018

Declaration

I declare that this written submission represents my ideas in my own words, and where ideas or words of others have been included, I have adequately cited and referenced the original sources. I also declare that I have adhered to all principles of academic honesty and integrity and have not misrepresented or fabricated or falsified any idea/data/fact/source in my submission. I understand that any violation of the above will be a cause for disciplinary action by the Institute and can also evoke penal action from the sources that have thus not been properly cited, or from whom proper permission has not been taken when needed.



(Signature)

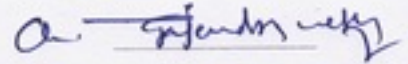
(Greeshma P. M.)

EE16MTECH1021

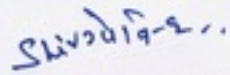
(Roll No.)

Approval Sheet

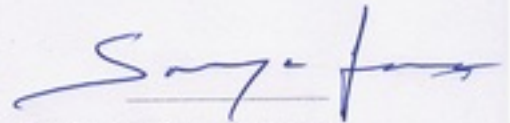
This Thesis entitled Fabrication of micro separation column for miniaturized gas chromatography system by Greeshma P. M. is approved for the degree of Master of Technology from IIT Hyderabad



(Dr. Gajendranath Chowdary) Examiner
Dept. of Electrical Engineering
IITH



(Dr. Shiv Govind Singh) Adviser
Dept. of Electrical Engineering
IITH



(Dr. Soumya Jana) Chairman
Dept. of Electrical Engineering
IITH

Acknowledgements

First of all, I would like to thank almighty for keeping me in good health and for all the grace. I would like to thank my mother for always being supportive.

I express my deepest gratitude to my guide prof. Dr. Shiv Govind Singh sir for his valuable guidance, constant support and motivation which helped me in the completion of my thesis. He was always there when I had doubts. His wisdom and guidance has led me path to achieve success in this project work.

I wish to thank all my colleagues and senior students in the lab for helping and supporting me a lot to finish this work.

I wish to sincerely thank my family and friends for keeping faith in me and encouraging me throughout my work.

Dedication

To my mother....

Abstract

The emphasis of this work is on the fabrication of a micro separation column for application in miniaturized gas chromatography system. The micro column was made by microchannels fabricated on the silicon wafer and sealed with a glass lid. The microchannels were fabricated by wet etching process and the channels were of length 2m , width 200 μm and depth 100 μm . The channels were closed by sealing with Pyrex glass. Silicide bonding was done for the bonding of silicon with Pyrex glass. Ti was used as an intermediate layer and bonded at a temperature of 377°C and a force of 1kN. During bonding Ti forms an alloy with silicon and forms Titanium silicide and this helps to bond the glass wafer with silicom wafer with microchannels etched on it.

Contents

| | |
|--|-------------|
| Declaration | ii |
| Approval Sheet | iii |
| Acknowledgements | iv |
| Abstract | vi |
| Nomenclature | viii |
| 1 Introduction | 3 |
| 1.1 Gas Chromatography | 3 |
| 1.2 Proposed work | 4 |
| 1.3 Thesis organisation | 5 |
| 2 Background and Motivation | 6 |
| 2.1 Conventional GC Systems | 6 |
| 2.2 Gas Chromatography Instrumentation | 7 |
| 2.2.1 Injector | 8 |
| 2.2.2 Separation Column | 8 |
| 2.2.3 Stationary Phase | 9 |
| 2.2.4 Column Heating Techniques | 9 |
| 2.2.5 Detector | 9 |
| 2.3 Overview of miniature gas chromatography | 10 |
| 3 Fabrication of GC column | 16 |
| 3.1 Introduction | 17 |
| 3.2 Fabrication process of micro GC column | 18 |
| 3.2.1 Micro channel fabrication | 18 |
| 3.2.2 Square spiral channel fabrication | 20 |
| 3.2.3 Circular spiral channel fabricarion | 22 |
| 3.2.4 Dry etching | 25 |
| 3.3 Bonding | 26 |
| 4 Appendix | 29 |
| 4.1 Acoustic separation of particles | 29 |
| 4.2 Background | 30 |
| 4.3 Device structure and Principles | 31 |

| | | |
|-------|---------------------------------------|-----------|
| 4.3.1 | Effect of tilted angle SSAW | 33 |
| 4.4 | Simulation and Results | 35 |
| 4.4.1 | Effect of tilted angle | 37 |
| | References | 42 |

List of Figures

Figure 2.1: Principle of elution chromatography

Figure 2.2: A sample chromatogram

Figure 2.3: Components of a Gas Chromatography system

Figure 2.4: Photograph of a MEMS GC system components [4]

Figure 2.5: Block diagram of the MEMS mGC prototype analytical system: (a) calibration-vapor source before (left) and after (right) assembly; diffusion channel and headspace aperture can be seen in the top section and macro-PS reservoir can be seen in the bottom section; (b) 3-stage adsorbent microPCF prior to loading and sealing (top left), with close-up SEM images of each section loaded with adsorbents (lower left) and assembled structure with capillary interconnects on a U. S. penny; (c) 3 m separation-column chip (left) with close up views of the channel crosssections prior to (top right) and after (lower right) sealing; (d) detector assembly with 4-chemiresistor array chip (right), Macor lid (white square structure), and sealed detector with connecting capillaries mounted on a custom mounting fixture (left). The dashed line is a flow-splitter [6]

Figure 2.6: Design of square-spiral column. Black and white stripes indicate the flow direction in adjacent channels. Details of connection line ports and gas flow direction is shown on the right [7]

Figure 2.7: Layout of the column with embedded micro-posts (left), SEM image of cross-section of semi-packed column (right) [9]

Figure 2.8: Micro GC with -separation column, TCD -Preconcentrator. SEM image showing the PDMS coating on the walls of the column channel [10]

Figure 2.9: (A) SEM and optical images of the DRIE channels of a micro-column fabricated in this research, (B) photograph showing the gold diffusion-bonded all-silicon micro-column packaged with Nanoports for chromatographic testing and (C) Scanning acoustic micrograph image of the channels of a micro-column die showing the absence of large voids at the interface of the gold diffusion-bonded silicon microchannels. The image shows the channel region (100 microns) in dark green color and bonded silicon regions in light orange-yellow color. [11]

Figure 2.10: a) SEM images of the bonded interface of gold eutectic bonded; b) Energy dispersive X-ray showing the Au richness around the bonded area; and c) Location of gold atoms at the interface, d) Location of silicon atoms, e) location of oxygen [4]

Figure 3.1: Mask for rectangular spiral channel

Figure 3.2: Mask for circular spiral channel

Figure 3.3: Process flow for microfabrication of channel

Figure 3.4: Inlet of square spiral channel after etching

Figure 3.5: Corners of square spiral channel after etching

Figure 3.6: Circular spiral channel after etching in 25 wt% TMAH and 0.4% v/v Triton X-100

Figure 3.7: Circular spiral channel after etching in 25 wt% TMAH and 0.4% v/v Triton X-100 for 2 hours

Figure 3.8: Circular spiral channel after etching in 25 wt% TMAH and 0.4% v/v Triton X-100 for 3 hours showing the difference in the width of the channels

Figure 3.9: Histogram showing the depth of the channels etched for 2 hours (top) and 3 hours (bottom)

Figure 3.10: 2D and 3D images taken using profilometer after RIE for square (top) and circular (bottom) spiral channels

Figure 3.11: 2D (top left), 3D (top right) and histogram (bottom) showing the depth of the square spiral channels etched in TMAH for 3 hours

Figure 3.12: Process flow for bonding of microfabricated channel and pyrex glass

Figure 4.1: Schematic of the SSAW based device showing separation and focusing

Figure 4.2: Schematic of the SSAW propagating along the surface of the piezoelectric substrate and extends to the channel

Figure 4.3: Acoustic radiation force along the channel on different particle sizes

Figure 4.4: Schematic diagram of the tilted SSAW separator showing the pressure and antipressure nodes as dashed lines [17]

Figure 4.5: orientation of particles with different sizes according to the orientation of pressure nodes and antipressure nodes

Figure 4.6: Total displacement plotted against frequency for finding resonant frequency

Figure 4.7: Acoustic pressure field generated in the channel region by the SSAW

Figure 4.8: Distribution of the pressure nodes when the IDTs are placed at different distance from the channel

Figure 4.9: Distribution of the pressure nodes when the IDTs are placed at a distance from the channel such that anti pressure nodes come in centre and pressure node comes at sides of the channel

Figure 4.10: Distribution of the pressure nodes when the IDTs are placed at a distance from the channel such that anti pressure nodes and anti pressure nodes will come at the sides of the channel and the channel will focus the particles

Figure 4.11: The trajectory of two particles with different diameters when introduced to a channel which focusses the particles.

Figure 4.12: The trajectory of two particles with different diameters when introduced to a channel which focusses the particles at different time instances at a time step of 0.1s .

Figure 4.13: The displacement of the particle with different diameters as the effect of the tilted Channel

Figure 4.14: The displacement of the particle with same diameter at different angles

Chapter 1

Introduction

1.1 Gas Chromatography

Chromatography is one of the most common analytical methods for separation and detection of different chemicals in a complex mixture. It is also used in preparative analysis where the aim is purification of a substance. Chromatography techniques can be used to detect the presence of a chemical in a mixture as well as to estimate the quantity of the component in the mixture. The principle behind the separation is the relative amount of each component distributed between a moving phase and a fixed phase. The moving stream of fluid is called mobile phase and the fixed phase is called stationary phase. Certain components in the mixture will favour the distribution in mobile phase while others favour stationary phase. The component which favours stationary phase will remain in the column for longer than the component which favours the mobile phase. So unlike the physical separation techniques like distillation, crystallization etc, chromatography creates a time separation.

Chromatography is widely used in biological as well as chemical fields. In biochemical researches this technique is used to identify and detect different chemical components. It is used in environmental analysis for the detection and quantification of pollutants in the atmosphere. Chromatography has industrial applications as well. In petroleum industry, it is used for detecting and analyzing various complex hydrocarbons. Chromatography techniques are also used in various industries for purification of commercial products. It has also got applications in forensic research, therapeutics research, explosives detection etc.

According to the physical state of the mobile phase, Chromatography is divided into liquid chromatography and gas chromatography. In liquid chromatography, the mobile phase will be a liquid whereas in gas chromatography, the mobile phase will be a gas. In both types of chromatography, stationary phase can be solid or liquid. Either it can be a liquid filled in the column or a coating of a solid on the walls of the column or a pack of solid. In all these types of chromatography, the type of interaction between analyte and the two phases will vary. The mechanism can be adsorption or intermolecular interactions. In gas chromatography, the gaseous analytes can be separated according to the boiling point, solubility, polarity, specific chemical interaction etc. Gas chromatography and high performance liquid chromatography are the most widely accepted analytic tools. They

have almost entirely replaced the other chromatography techniques. HPLC technique is used in the analysis of organic acids where as GC techniques are used in analysis of volatile components.

Gas chromatography is a technique used in analytical chemistry to separate volatile and semi-volatile components in a complex mixture [1]. It is a widely accepted separation technique due to its simplicity, sensitivity and separation efficiency. The separation mechanism is mainly the difference in boiling point or the vapor pressure and the polarity. The mobile phase in gas chromatography will be an inert gas. The stationary phase can be a solid or a viscous liquid. In gas-liquid chromatography, the separation is based on the partitioning of the volatile analyte between the inert carrier gas and the non-volatile liquid coated on an inert surface. In gas-solid chromatography, the separation is based on the selective adsorption of the different sample constituents on a solid stationary phase.

Gas chromatography is a widely accepted technique in analysis of hazardous air pollutants in atmosphere [1]. Many chronic diseases and health hazards can be caused by increased rate of air pollution. Analysis and detection of toxic and hazardous components in environment can be made easy using GC. Due to high sensitivity and efficiency of GC equipment, very small traces of these components in atmosphere can be detected and quantified.

Miniaturization of GC systems has been explored by researchers since the introduction of GC. Considerable interest has been showed by researchers to develop a low power, low cost and portable GC system [2]. Miniaturizing not only makes the device portable but reduces the analysis time as well as the amount of analyte requires in a sample. As the quantity of sample required is very less in a micro GC system, it will bring considerable advantages in biological research and environmental analysis. With micro GC systems, even traces of the analytes in the sample can be detected and quantified. This advantage can be exploited in the detection of air pollutants, explosives detection, pathogen detection, volatile organic compound detection etc. Currently, much efforts have been made in developing microfabricated components and optimizing these components. Developing high performance microfabricated components is a challenge in miniaturizing GC systems. Batch fabrication, sensitivity, and lower cost are also limitations of the currently developed systems.

1.2 Proposed work

The aim of this thesis is to develop a miniaturised gas chromatography channel. Fabrication of a micromachined channel on silicon for micro GC application is investigated in this work. A new bonding technique is introduced in this work to bond the silicon wafer with channels fabricated for GC and a Pyrex glass to cover the channels. Silicide bonding is used where Ti is used as the intermediate layer for bonding. A low temperature and pressure bonding is achieved.

1.3 Thesis organisation

Chapter 1 is the introduction to chromatography and gas chromatography. It also explains the proposed work.

Chapter 2 explains shortly about conventional and miniaturized gas chromatography systems. It also gives a brief history of the miniaturized gas chromatography systems and micro separation columns.

Chapter 3 explains the fabrication process of the micro separation column and bonding of the column wafer to seal the microchannels.

Chapter 4 is the appendix, which explains another work done by me. This focuses on the separation of particles based on acoustic field. This chapter shows simulation details and results of the acoustic based separation process.

Chapter 2

Background and Motivation

This chapter briefly explains the principle of gas chromatography, conventional gas chromatography systems and micro GC systems. The components of the GC system and the miniaturization of the components are also explained.

2.1 Conventional GC Systems

The most common GC technique used to separate and quantify volatile components in a mixture is elution chromatography. A stream of inert gas containing the sample mixture is passed through a column which is coated with a viscous liquid stationary phase. When the sample passes through the column, different components in it will interact with the stationary phase. Some components will have more affinity to the stationary phase and they prefer to stay in stationary phase for more time compared to components with less affinity to the stationary phase. These will take more time to come out of the column. The components which have less affinity to stationary phase will prefer to stay in the carrier gas medium and will pass out of the column easily. So a separation in time can be obtained between different components in the mixture. This principle is illustrated in Fig. 2.1. A mixture of three components A, B and C is passed through a chromatography column. Compound C which has least affinity to the stationary phase coating is the one to leave the column at first. Compound A which has highest affinity to the stationary phase will leave the column at last. Compound B will come out at a time between the other two. The separation happens in time. The detector will produce a signal which shows the time at which each compound left the column. This detector signal plot in time is called a chromatogram. A sample chromatogram for the separation process shown in Fig. 2.1 is shown in Fig. 2.2. Each peak in the chromatogram shows the time at which the compound left the column. Chromatogram can not only be used for detecting different components but also to quantify the amount of the particular component in the mixture. The area under every peak gives the quantity of the compound present in the mixture.

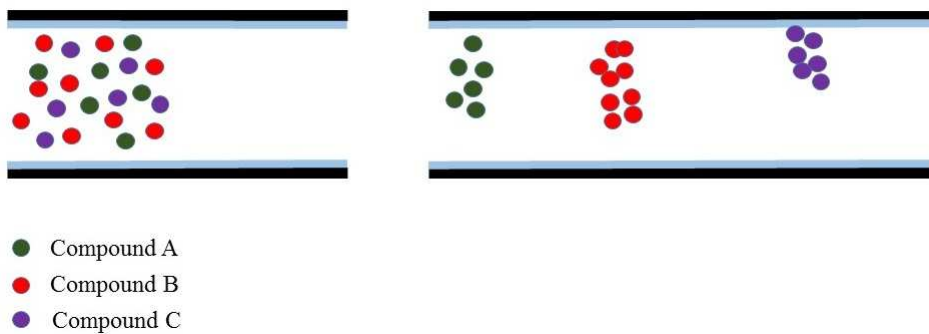


Figure 2.1: Principle of elution chromatography

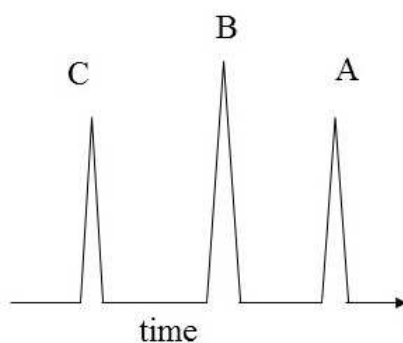


Figure 2.2: A sample chromatogram

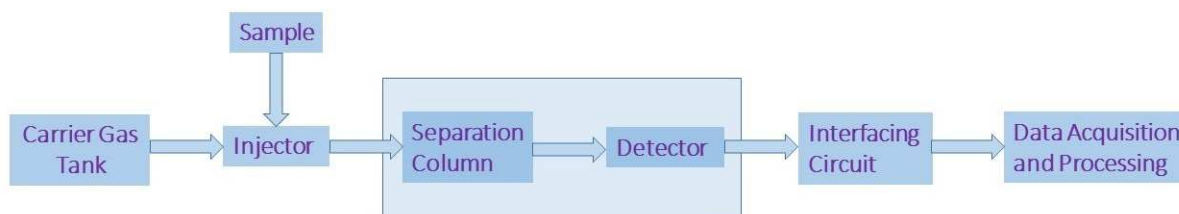


Figure 2.3: Components of a Gas Chromatography system

2.2 Gas Chromatography Instrumentation

The conventional gas chromatography system has different components assembled together to achieve the separation as well as detection and interpretation. Figure 2.3 shows the block diagram of the GC system. For a miniaturized version of a conventional GC system, each of these components should be miniaturized and integrated to form a portable device. The coming sections explain different components of a GC system.

2.2.1 Injector

The purpose of the injector is to introduce a very small amount of sample into the column. The injector is normally kept at a high temperature to make sure that all the components are in gaseous state. Sampling valves, preconcentrators etc are used as injectors. Fast and repeatable injections of samples into the column directly affect the column efficiency. An injector with a small dead volume and very fast valve is necessary to prevent band spreading and poor resolution [3]. Split or splitless injectors are used in conventional systems to inject very small amount of sample to the column. A heating apparatus will also be accommodated to heat the sample and vaporize it before injection.

2.2.2 Separation Column

Separation column is the heart of GC. It is the most important part of GC which affects the overall performance and efficiency of the GC system. The whole separation takes place in the column. Conventional bench top systems use separation columns of length ranging from 10 to 60 m. There are different types of columns used.

Packed columns

Packed columns are having 2-10 meters length and 2-4 mm internal diameters. These tubings are usually made up of glass, stainless steel or plastic and will be packed with some inert material. The packing inside the tubings will be finely divided solid support material which is inert. This packing material will be coated with the stationary phase coating. Packed columns increase the surface area for interaction with the components in the separating mixture and increases the efficiency of the separating column [1]. Packed columns are mostly used for the separation of volatile gaseous mixtures. Packed columns need more amount of samples. In earlier times, with less sensitive detectors, packed columns were necessary. However, with modern high sensitivity detectors, packed columns are not used as the amount of sample required is very less.

Capillary columns

Capillary columns are the most commonly used separation column which will be having lengths ranging from 10-60 m. These will be having very less inner diameters which will be normally in the range of some hundreds of micrometers. Mostly the capillary columns are made up of fused silica with a flexible polyimide coating which gives strength and protection to the fused silica inside. Usually these flexible columns are wound to a small coil form inside the chamber. The inner walls of the tubing will be coated with the stationary phase coating. Before coating the stationary phase, the inner walls of the tubing will be inactivated to avoid any possible chemical interactions. Capillary columns produce very narrow peaks and this allows the separation of very complex mixtures like petroleum products etc which contains enormous number of hydrocarbons in it. Capillary columns require very small amount of samples when compared to packed columns. So these are now commonly used with modern high sensitivity detectors which require very less quantity of sample. So these are very useful in environmental as well as biological analysis.

2.2.3 Stationary Phase

Stationary phase is the key component in A GC system. This coating inside the separation column which reacts with the components in the gaseous mixture and is responsible for the separation. So, the quality of stationary phase coating will directly affect the separation efficiency of the column. Different thickness of the coating and the type of the coating affects the separation. The polarity of the solute and the stationary phase affects the separation. There are two types of stationary phases, polar and non polar stationary phase. Non polar stationary phases are dimethyl polysiloxane, hydrocarbons, dialkyl siloxanes etc. Polyester coatings are polar stationary phases. The sample polarity should always match the stationary phase polarity. There are two methods for coating the stationary phase: static coating and dynamic coating. The inlet and outlet of the channel will be connected to a tubing and coating material is pumped into the channel. One end of the channel is connected to a vacuum pump and placed on hot water or isothermal oven. The solvent evaporates leaving a thin layer of coating on the walls of the channels. The uniformity of the coating depends on the smoothness of the channel walls.

2.2.4 Column Heating Techniques

Temperature is a very important factor that affects the separation performance of the column. By controlling temperature the separation can be easily controlled. Temperature can be controlled by heat transfer phenomenon such as conduction, convection and radiation. These ovens have high internal volume and thermal mass. The time required to reach the desired temperature is also high. This is not suitable for a portable application.

Infrared heating is also used to heat the column. Electromagnetic waves are used in this technique. Resistive heating is another technique. A resistive element is integrated to the column and electric current is passed through the heating element. Lower power consumption and faster heating are the advantages of this joule heating technique.

2.2.5 Detector

Detectors are the most important part of a GC system. An ideal detector should be non destructive, highly sensitive, low power consuming and fast response. The amount of analyte required for the detection should be less. Most popular detectors are flame ion detector, Thermal Conductivity detector and Electron capture detector. FID uses a mixture of a combustible gas and air to form a flame above the burner and measure the current generated across the electrodes and nozzle due to ionized combustion products. But these are not suitable for portable applications. ECD are used for halogen containing compounds that are hard to detect. Chemiresistive detectors, mass spectrometers are also used as detectors with GC systems. TCD uses the change in thermal conductivity of different components passing over the detector. These can be used in portable systems due to fast response, simplicity, low cost etc.

2.3 Overview of miniature gas chromatography

Conventional GC systems are bulky because of the incorporation of a heating oven chamber, carrier gas tanks etc. They are more power consuming and have slow response leading to high analysis time. The temperature control in these are also difficult. These systems are not portable and they cannot be used for field applications. The use of these are limited to laboratory and the sample has to be collected from the field and then carried to the laboratory. Advances in MEMS technology introduced miniaturization in many fields. This influenced the miniaturization of laboratory equipments also. GC system can also be miniaturized to a complete analysis portable system with the help of MEMS technology.



Figure 2.4: Photograph of a MEMS GC system components [4]

A microfabricated GC system mainly has miniaturized pump, miniaturized valve, microchannel and a micro detector. This forms the miniaturized components of the microGC system. Along with these interfacing circuitry and a processor should also be there. Figure 2.4 shows the photograph of a microGC system components assembled together by researchers in Georgia Institute of technology [4]. Miniaturization of GC systems started since it was introduced by Terry [5] in 1970. This was the first attempt to miniaturize GC system. This work consisted of a 1.5 m spiral capillary column with a width of 200 μm and depth of 30 μm . The channel was having an approximately rectangular cross section. The channel was anodically sealed with PYREX glass lid. A miniature solenoid actuated diaphragm valve etched on silicon was used for sample injection. Detection was done by a nickel resistor thermal conductivity detector. This system was able to do the separation in 10 s. After that many attempts has been done for improving the efficiency of the miniaturized system. In 1998, Sandia National Laboratories reported on open-tube columns with rectangular channels.¹⁹ This column separates a single component from a mixture

First generation hybrid MEMS GC was introduced successfully by Chia-Jung Lu [6]. This system was capable of separating 11 vapour mixture of air in less than 90 s with a detection limit of 5-36 ppb in 0.25 L. Figure 2.5 shows the block diagram and components of the first generation

hybrid MEMS GC. It consisted of a calibration vapour source, multistage preconcentrator, 3m micromachined separation column, chemiresistor based detection system. This was the first study to demonstrate the quantitative analysis of a mixture of vapors by a MEMS GC. In this work, the separation column was etched by DRIE in silicon and sealed by anodic bonding.

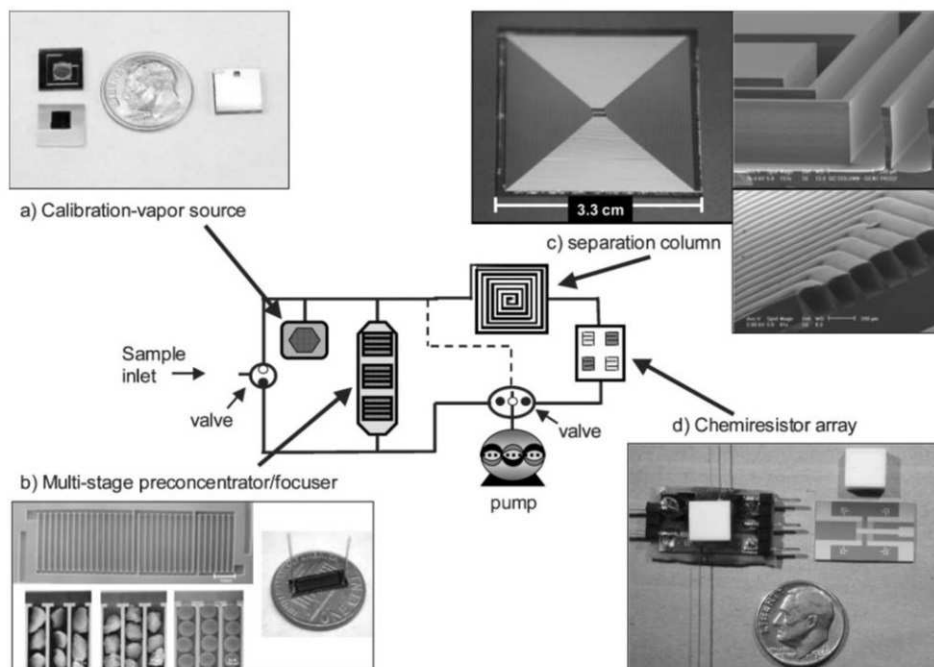


Figure 2.5: Block diagram of the MEMS mGC prototype analytical system: (a) calibration-vapor source before (left) and after (right) assembly; diffusion channel and headspace aperture can be seen in the top section and macro-PS reservoir can be seen in the bottom section; (b) 3-stage adsorbent microPCF prior to loading and sealing (top left), with close-up SEM images of each section loaded with adsorbents (lower left) and assembled structure with capillary interconnects on a U. S. penny; (c) 3 m separation-column chip (left) with close up views of the channel crosssections prior to (top right) and after (lower right) sealing; (d) detector assembly with 4-chemiresistor array chip (right), Macor lid (white square structure), and sealed detector with connecting capillaries mounted on a custom mounting fixture (left). The dashed line is a flow-splitter [6]

GC column design is based on compromises between analytical requirements and engineering constraints for microfabrication. Double square spiral channels were introduced for reduced size of the channel die and more efficiency by increasing length of channel. The two parallel channels are indicated in black and white. Flow direction is opposite in adjacent channels. The channels meet at the center of the chip by means of two unetched posts, which act as flow barriers [7]. The schematic of double square spiral channels are shown in Fig. 2.6.

Agah et al. [8] has demonstrated a high speed MEMS based GC with temperature programming. They demonstrated the separation of an eleven compound mixture in few seconds. They integrated a microfabricated silicon separation column, resistive heaters, temperature sensors, and capacitive pressure sensors. The 25 cm long 150 μm wide and 250 μm deep columns were fabricated on silicon

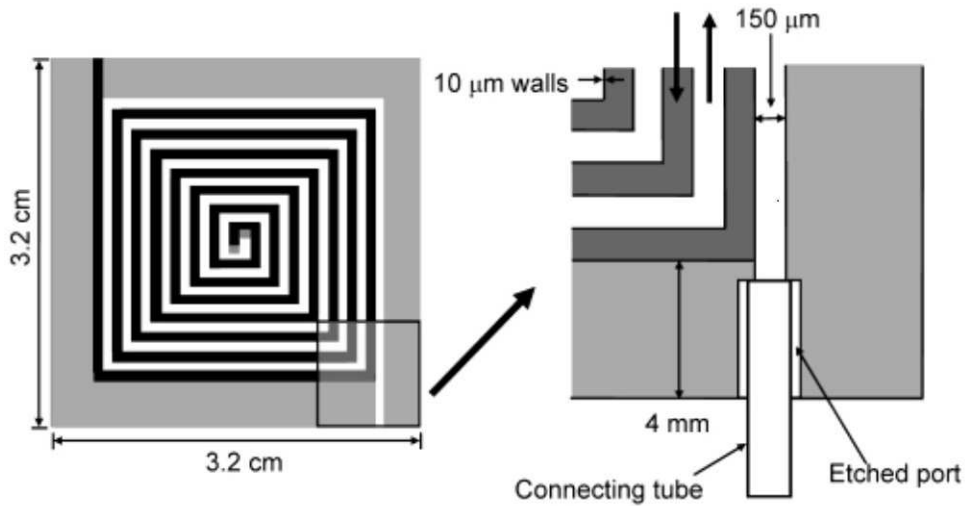


Figure 2.6: Design of square-spiral column. Black and white stripes indicate the flow direction in adjacent channels. Details of connectionline ports and gas flow direction is shown on the right [7]

wafer and sealed with glass by anodic bonding. Integrated heaters, pressure sensors and temperature sensors were used to give temperature programming. Temperature ramp of $10^{\circ}\text{C}/\text{s}$ was obtained. They demonstrated the separation of an eleven component mixture in less than 10 s.

Yi Li et al. [9] has fabricated micro GC columns through MEMS fabrication technique with improved column efficiency. Two types of columns were designed. An open tubular column and a semi packed column. They reported that the efficiency was improved by embedding square posts in the channel to form semi packed column. The plate number was five times higher than the value reported previously with other MEMS GC systems. Column with 1 m length, $160\ \mu\text{m}$ width and $250\ \mu\text{m}$ depth were formed by DRIE. The square posts were embedded into the channels. Two square posts which were at a distance of $40\ \mu\text{m}$ were embedded and a layer of such posts were added at a distance of $40\ \mu\text{m}$. This increased the overall surface area and hence the efficiency. The column was sealed by Pyrex glass by anodic bonding.

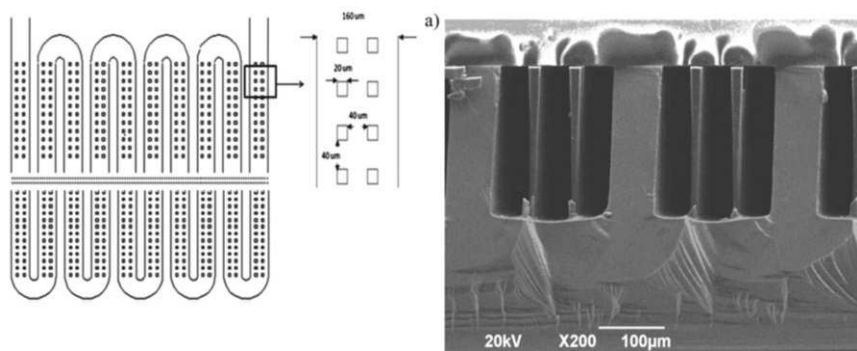


Figure 2.7: Layout of the column with embedded micro-posts (left), SEM image of cross-section of semi-packed column(right) [9]

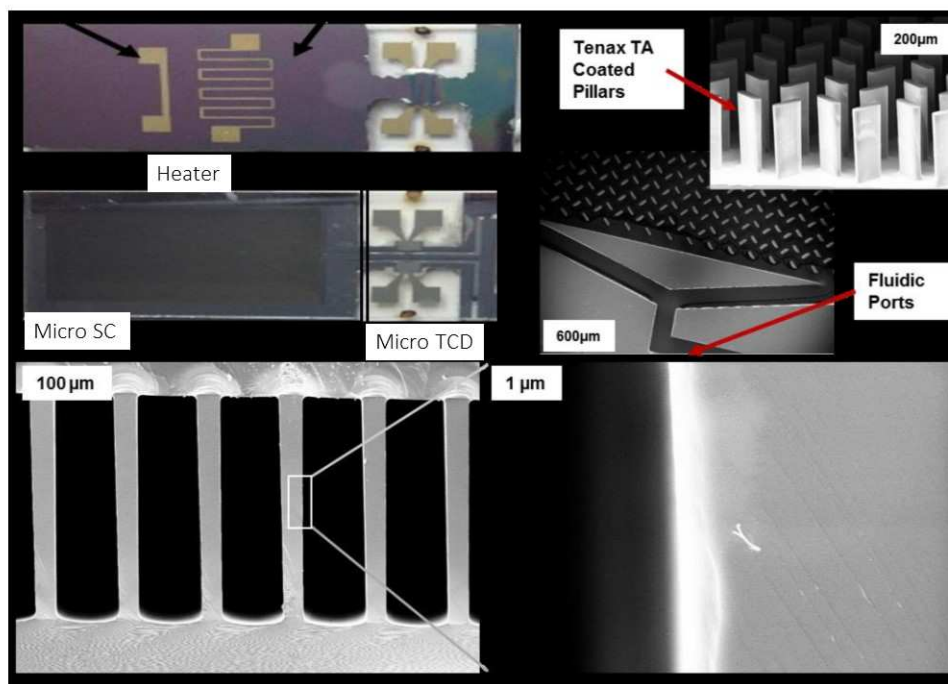


Figure 2.8: Micro GC with μ -separation column, μ TCD μ -Preconcentrator. SEM image showing the PDMS coating on the walls of the column channel [10]

Garg et al. [10] have demonstrated implementation of a microfabricated gas chromatography system specialized for detecting hazardous air pollutants (HAPs) at ppb concentration level. A MEMS separation column with an on-chip thermal conductivity sensor, and a micro preconcentrator were integrated for separating and detecting benzene, toluene, tetrachloroethylene, chlorobenzene, ethylbenzene, and pxylene. This work demonstrated the use of a micro fabricated preconcentrator which will act as an injector. Micro posts or fluidic ports were etched on silicon and were coated with Tenax TA solution. The chip was then capped with Borofloat wafer by anodic bonding. Heaters were fabricated by depositing and patterning metal layer on the back side of the same wafer. The micro separation column was fabricated on silicon wafer with a two step anisotropic etching for the inlets and channels. DRIE was done to create $200\ \mu\text{m}$ deep rectangular channels. Micro TCD was fabricated by depositing and patterning metal and etching out a step from the insulator. They have reported a limit of detection (LOD) of $1\ \text{ng}$ with sampling time of $10\ \text{min}$ at a flow rate of $1\ \text{mL}/\text{min}$, and they showed 3 orders of magnitude lower sample volume as compared to the conventional GC system.

Radadia et al. [11] has reported the fabricatiuon of an all silicon micro GC columns. They introduced an all silicon miro separation channel for the first time. They avoided the use of yrex glass as the material for sealing the column. They reported the use of silicon wafer itself for the sealing of micro channels. For bonding the etched channel wafer with the lid wafer they used gold as an intermediate metallic layer. Eutectic bonding was used for bonding. Gold was sputtered to the lid wafer surface and bonded to the wafer with the microchannels etched. The etched channels wrer $100\ \mu\text{m}$ wide and $100\ \mu\text{m}$ deep and $34\ \text{cm}$ long. A six component mixture of n- alkanes were

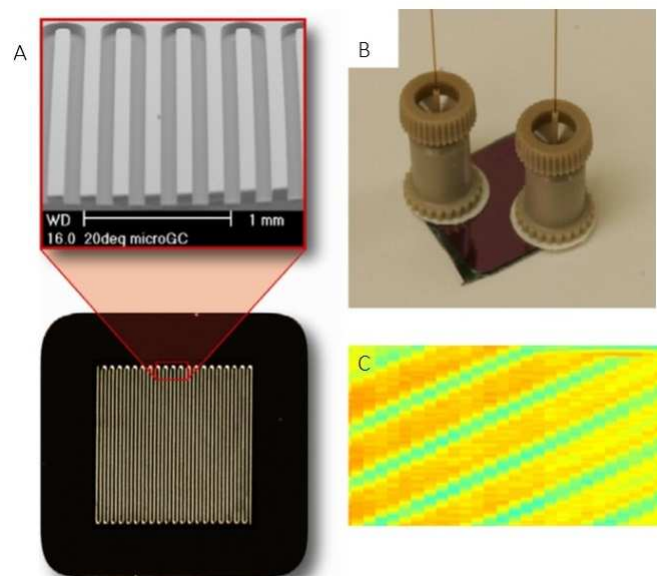


Figure 2.9: (A)SEM and optical images of the DRIE channels of a micro-column fabricated in this research, (B) photograph showing the gold diffusion-bonded all-silicon micro-column packaged with Nanoports for chromatographic testing and (C) Scanning acoustic micrograph image of the channels of a micro-column die showing the absence of large voids at the interface of the gold diffusion-bonded silicon microchannels. The image shows the channel region (100 microns) in dark green color and bonded silicon regions in light orange-yellow color. [11]

separated in 30 s. Later lower separation times were reported with long channels and higher flow velocity.

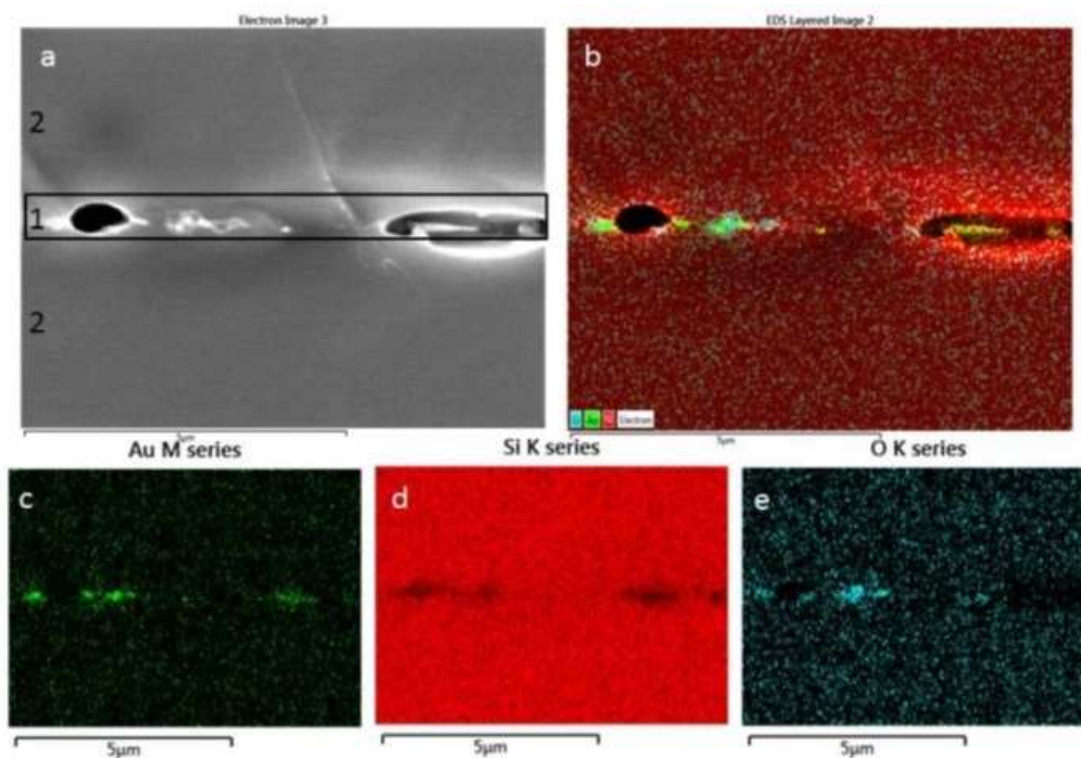


Figure 2.10: a) SEM images of the bonded interface of gold eutectic bonded; b) Energy dispersive X-ray showing the Au richness around the bonded area; and c) Location of gold atoms at the interface, d) Location of silicon atoms, e) location of oxygen [4]

Navei M. et al [4] introduced a gold Eutectic fusion bonding for the fabrication of an all silicon micro GC column. To improve the bonding efficiency in [allsi] they reported that by annealing the eutectic bonded silicon wafers at the eutectic temperature, the bond strength will be improved. The microchannels were etched on silicon with DRIE to a depth of $300\ \mu\text{m}$ and $75\ \mu\text{m}$ width. The columns were fabricated for two lengths, 3m and 2m. The inlets were also etched on the channel wafer by back side alignment and etching. The top lid wafer was coated with 100 nm gold by evaporation and bonded at $420\ ^\circ\text{C}$ and 10 MPa. The eutectic bonded dies were then annealed at $1200\ ^\circ\text{C}$ for 2 hours in inert ambient. The work reported that formation of gold silicon alloy improves the bond strength and reduce stress. A six component mixture was separated in less than 10 s. This device was then integrated with temperature programmed heater fabricated on the other side of the lid wafer, and micro TCD detector for analysis of volatile organic compounds.

Chapter 3

Fabrication of GC column

This chapter explains the process of fabrication of the micro GC column on Silicon wafer. A high efficiency micro GC system is achievable only with a high performance micro GC column. The separation efficiency, speed of separation etc of the system is directly dependent on the micro GC column. Proper separation of the components in a complex mixture is the essential process in gas chromatography. The detection and quantification is possible only if separation efficiency is high and this is achieved only when the micro column performance is high. The micro GC column should be able to withstand the pressure variations and the temperature cycling of the system. So for a lab on a chip system for any application such as environmental analysis, pathogen detection, biological analysis, purity test etc, the overall performance depends on the micro GC column performance. For a miniaturized system, the micro column should be of least possible size with high performance. This work shows a fabrication process of a micro GC column fabricated on a silicon wafer and closed with a pyrex glass lid.

3.1 Introduction

The micro GC column is the heart of micro GC system. Micro GC columns are fabricated by etching High aspect ratio channels in silicon wafer and sealing them with a lid, either pyrex glass or silicon wafer. The etched channels can be laid in circular spiral or square spiral for forming the separation column. The micromachined column closed with the lid has to be then coated with the stationary phase like polydimethyl siloxane, to which the components in the mixture will interact.

The etching of the microchannels is normally done by deep reactive ion etching. The channels should be of very high aspect ratio and with smooth side walls. Due to the unavailability of the DRIE system, in this work, we have used wet etching process. DRIE will provide high aspect ratio and thus deeper channels with less width can be obtained by using DRIE process. The deeper the channel, the lesser can be the width which will reduce the size of the chip. For miniaturized GC systems, high performance column with smaller overall dimensions have to be fabricated. This reduction in dimension can be obtained by increasing the depth of the channel by reducing the width of the channel. The lesser the width, more will be the efficiency. Also smoother sidewalls are possible with DRIE. The roughness in the channel walls will adversely affect the uniformness of the stationary phase coating. Due to these reasons DRIE is preferred in microchannel fabrication. For improving efficiency channels can be fabricated by DRIE later, once the bonding process is evaluated. In this work wet etching in TMAH is done for fabricating channels on silicon.

Once the fabrication of the channel is done, these should be closed with suitable material. Pyrex substrate is widely used as lid to close the micromachined channels. Bonding a high density micromachined surface is very difficult to achieve. There are several techniques developed for bonding and sealing the MEMS micro GC columns. Anodic bonding, eutectic bonding, fusion bonding are the widely used bonding techniques.

Anodic bonding [8] is the widely used and well developed process for sealing the micro channels with pyrex lid. Here bonding is done without the use of an intermediate layer and direct bonding of silicon and pyrex is done. Among the various bonding methods available, anodic bonding is a low cost and easily achievable bonding with good bond strength. But the major problem in anodic bonding is the difference in thermal conductivities of the materials. The thermal conductivities of the silicon and pyrex varies to a greater extent and this may cause fatigue cracking and cause non uniform temperature profiles.

Fusion bonding is another technique which bonds silicon onto silicon. Fusion bonding technique also doesn't use an intermediate layer. The direct bonding of micromachined silicon channel wafer to another wafer is done. This technique is not well accepted and widely used for sealing micro GC columns. Eventhough it is a low cost and easy process, the high surface roughness is a drawback of this technique. The rough surface of the wafer with channel fabricated on it makes fusion bonding difficult and researchers have found it to be not a consistent method. The contamination of the wafer surfaces also creates problem in fusion bonding. The surface should be extremely clean and should possess high smoothness. For a micromachined wafer it is difficult to achieve this.

Eutectic bonding [11] is another technique which can be used for sealing micromachined channel. Eutectic bonding can be used to bond silicon to silicon as well as glass to silicon. This technique uses an intermediate layer

3.2 Fabrication process of micro GC column

3.2.1 Micro channel fabrication

The channel fabrication was done on a single side polished 4 inch diameter p type silicon wafer. The wafer was cleaned and 1 um thick oxide was grown. 1 um thick silicon dioxide layer was grown in order to make it act as a mask layer during the wet etching process. Proposed plan was to fabricate both square spiral as well as circular spiral channels. The masks for both rectangular and square spiral channels are shown in Fig.3.1 and Fig. 3.2 respectively.

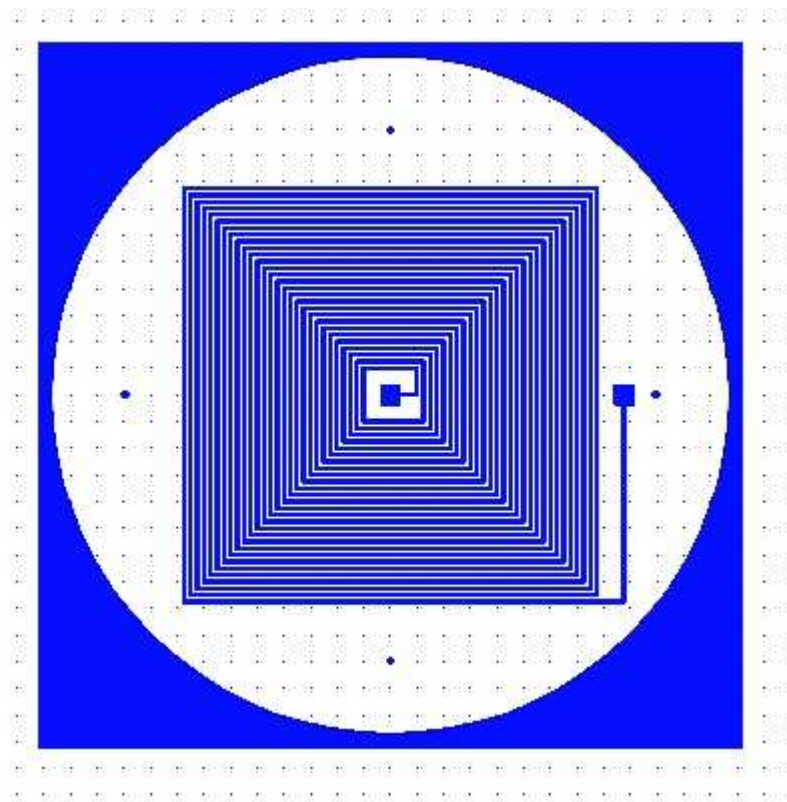


Figure 3.1: Mask for rectangular spiral channel

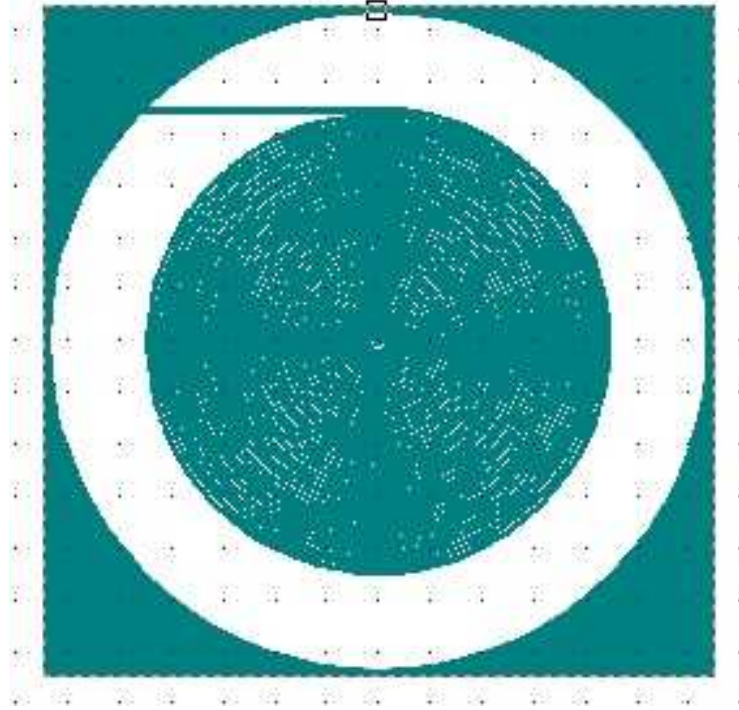


Figure 3.2: Mask for circular spiral channel

The rectangular spiral mask was designed in mask designing software CleWin 4. Clewin is a layout editor primarily developed for the design of MEMS. CleWin uses the Caltech Intermediate Format (CIF) as its native file format. CleWin can read and write GDS-II files also. The circular spiral mask was designed in Autodesk AutoCAD[®]. The masks were then wrote on to glass plates using laserwriter [name of m/c]. For writing the masks, 3 inch X 3 inch glass plates were used. The glass plates were cleaned using piranha solution heated at 90 °C for 10 mins and dried. The cleaned plates were then deposited with a 100 nm layer of Titanium(Ti) using electron beam evaporator. These Ti coated plates were then spin coated with positive photoresist (PPR) S1813 (3000 rpm for 40 s) and baked at 115 °C for 1 min. The PPR and Ti coated glass plates were then mounted to the laserwriter. The mask will be transferred to the glass plate. After finishing the mask writing process, the PPR was developed by MF319 developer. After development, the PPR from exposed portions will be removed. This glass plate was then dipped into Ti etchant (HF:H₂O₂: DI water in the ratio 1:1:20). Then Ti layer will be removed from the exposed portions leaving those portions transparent to exposure. After that the PPR layer was removed by rinsing in acetone followed by IPA (Iso propyl alcohol) and the mask plate was then dried.

The oxidised silicon wafers were cleaned using piranha solution heated at 90 °C for 10 mins and dried. Then the cleaned and oxidised wafers were then spin coated with PPR S1813 at 3000 rpm for 40s, keeping ramp up and ramp down as 500 rpm for 10s each. This coated wafer was baked at 115 °C for 1 min. This was then lithographically exposed using the previously prepared mask to print the channels, inlet and outlet. After exposure, the sample was developed using PPR developer MF319 for 30s. After development, the wafer was left with PPR wherever the channels are not there. Oxide layer was exposed from the areas where the channels have to be formed. To etch

channels on silicon, the oxide has to be removed from these areas and this was done by dipping the wafer in buffered HF solution. During this process the oxide was protected wherever the PPR was remaining. After etching out the silicon dioxide layer, the PPR layer was removed by rinsing in acetone followed by IPA.

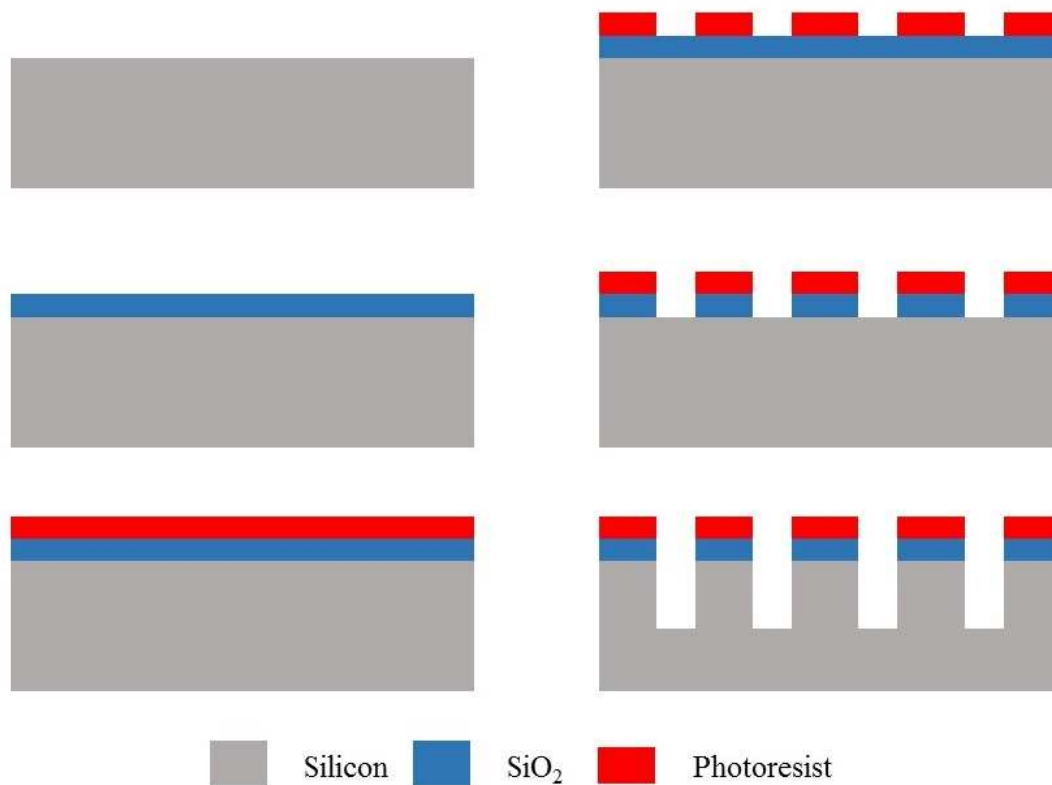


Figure 3.3: Process flow for microfabrication of channel

3.2.2 Square spiral channel fabrication

The wafer patterned with square spiral channels was etched by wet etching technique. 25% Tetramethylammonium hydroxide is used for wet etching of silicon. The patterned wafer was protected by oxide at the places where channels are not there and oxide was removed from wherever channels has to be etched. TMAH solution without dilution was taken for this etching process. The TMAH solution was taken in a flask which was sealed at the top. This was immersed in a water bath. A beaker filled with water was placed on a hot plate and the flask was immersed into it. The mouth of the flask was attached to a condenser. Water was used as the coolant in the condenser. The condenser was used to condense the evaporated TMAH so that the composition of the solution remains unchanged throughout the etching process. A temperature control mechanism was introduced to this system by immersing a sensor into the water bath and setting the temperature at 90 °C on the hot plate. The level of water in the waterbath was always kept above the level of TMAH in the

flask. When the temperature reached the desired setpoint, patterned wafer was placed on a wafer holder and immersed into the flask with TMAH solution.

The etch rate of the solution was found to be an average of $35 \mu\text{m/hr}$. The etching was performed for 3 hours. After 3 hours, the wafer was taken out from the TMAH flask and rinsed with DI water. The wafer was then dried and the etched channels were observed on the wafer. The depth of the channels were measured using optical microscope (OLYMPUS). Average depth was found to be $100 \mu\text{m}$. The edges were not as smooth and corners were observed to be not perfect. Figure 3.4 and Fig 3.5 shows the irregularities in the corners and edges of the pattern due to the wet etching process.

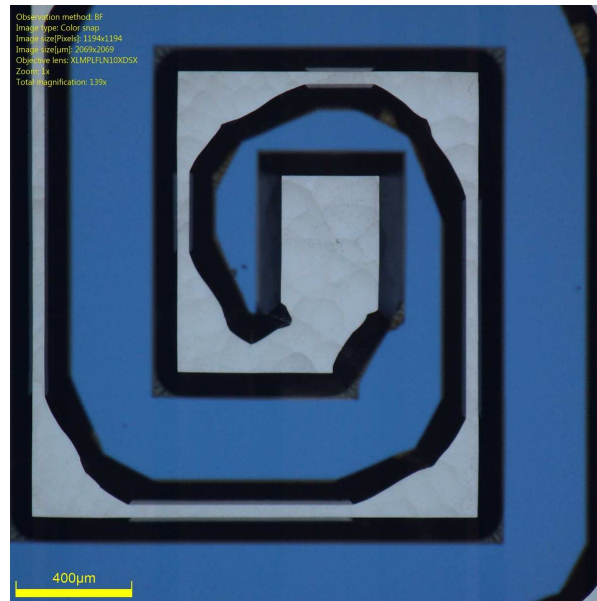


Figure 3.4: Inlet of square spiral channel after etching

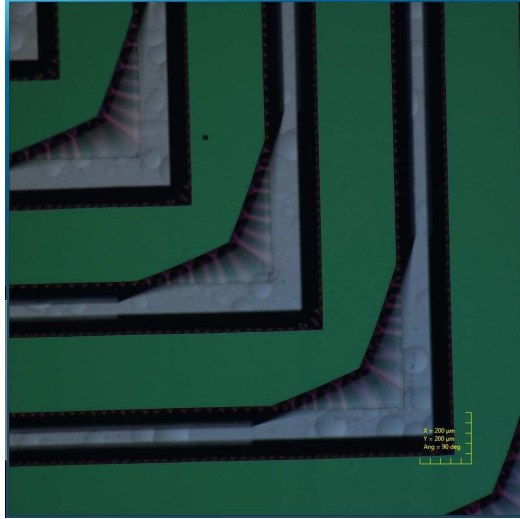


Figure 3.5: Corners of square spiral channel after etching

3.2.3 Circular spiral channel fabricarion

The circular spiral channel patterned on the wafer was also etched using TMAH. As TMAH etching cannot give perfect circular patterns [12], TMAH with Triton X-100 [13] was used. TMAH is used in Si bulk micromachining because of its compatibility with complementary metal oxide semiconductor (CMOS) process. It is well popular because of the benefit of using silicon oxide as a mask. TMAH has very good selectivity between silicon and silicon oxide. Due to this high selectivity between these, silicon oxide can be used as a mask layer for wet etching process using TMAH. Many researchers has been investigated the different etching behaviours of TMAH with different additives such as IPA, NC-200, Triton X-100 [13] etc. The additives helps in selective etching of different planes of silicon. Also additives enhance the etch rate of the process. Undercutting at convex corners, smooth finish at the etched surface can also be achieved by using additives.

When a circular pattern is etched using TMAH solution, it can result in a square structure after along etching duration. This happens because of different etch rate of TMAH across different planes in silicon. Etch rate for $\{110\}$ and $\{111\}$ planes are different for TMAH. For a structure different from square and rectangle, the etch surface will meet different planes during etching. The etch surface and the sidewalls will be of two different planes. This causes different etch rate and results in a deformation in the structure to be made. Reserches has been shown the use of mixture of IPA and KOH for formation of 3d circular structure [ref 3d]. But all these processess are used for very less depth. In this work, we have used TMAH and triton mixture for etching circular spiral pattern.

Triton was added to 25 wt % TMAH at 0.25 % v/v. The etching was done in the same apparatus explained in section 3.2.2. The rate of etching will change when triton was added. When a surfactant is added to TMAH, the surfactant exhibits a high tedency to adsorb onto 110 and its vicinal planes. This will strongly reduce the etching rate of 110 and its vicinal planes. As these surfactants has very less effect on 100 and its vicinal planes, the etch rate of these planes are not affected much by the surfactants.



Figure 3.6: Circular spiral channel after etching in 25 wt% TMAH and 0.4% v/v Triton X-100

The etched channels after 1 hour of etching is shown in Fig. 3.6. The pattern was not much deformed but the edges were having roughness and the edges were not smooth. The depth obtained after 1 hour of etching was $30\mu\text{m}$. So the sample was again etched for 1 hour in the same solution and same conditions. After 2 hours the sample was again checked under the microscope and the patterns obtained are shown in Fig. 3.7.



Figure 3.7: Circular spiral channel after etching in 25 wt% TMAH and 0.4% v/v Triton X-100 for 2 hours

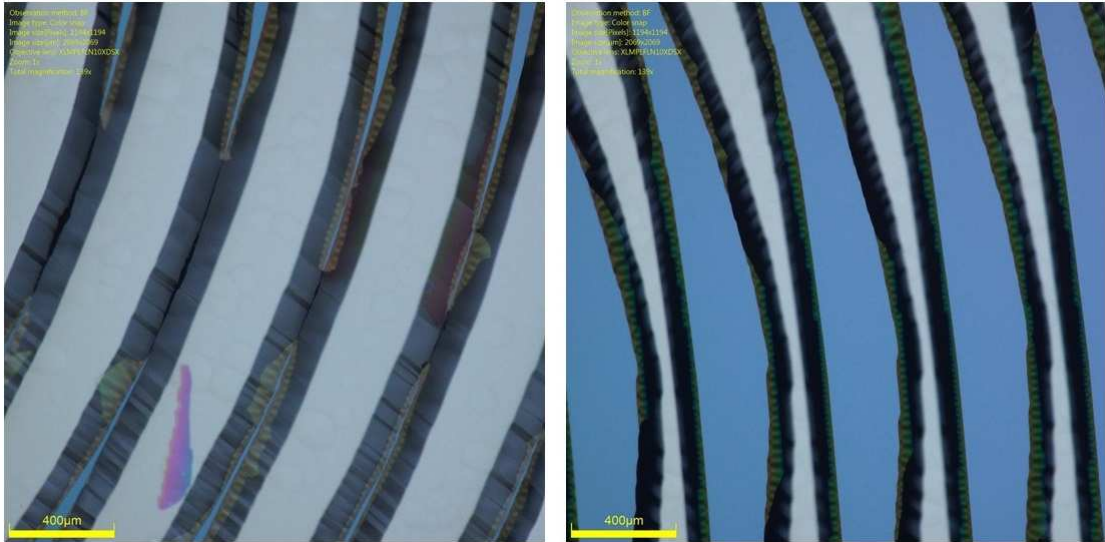


Figure 3.8: Circular spiral channel after etching in 25 wt% TMAH and 0.4% v/v Triton X-100 for 3 hours showing the difference in the width of the channels

After 2 hours, the channels width was found to be increasing and the depth was $66 \mu\text{m}$. Again the sample was etched for 1 hour and the channels obtained are shown in Fig. 3.8. There was a difference observed in the width of the channel at different sides of the channels. It was found that this technique cannot be used for the formation of deeper circular channels by etching silicon. Figure 3.9 shows the depth of the channels after 2 and 3 hours of etching.

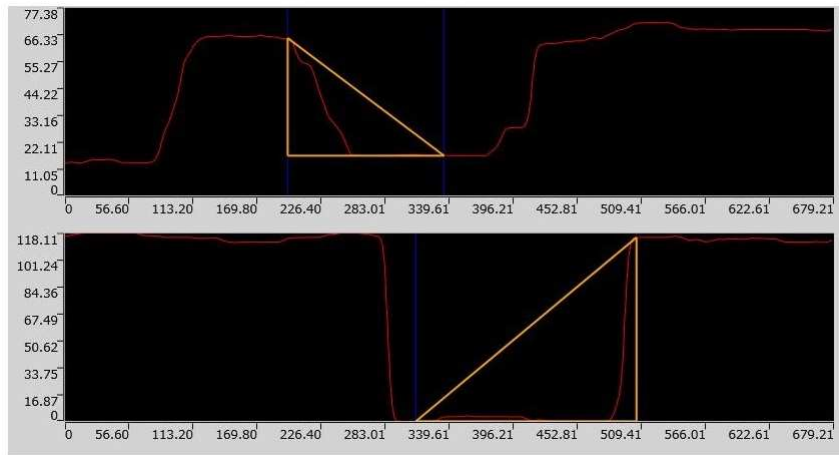


Figure 3.9: Histogram showing the depth of the channels etched for 2 hours (top) and 3 hours (bottom)

3.2.4 Dry etching

Dry etching was also done for fabricating the channels on silicon wafer. Dry etching is the best method for fabrication of 3D structure. Reactive Ion etching gives patterns with better surface roughness and accuracy.

As deep RIE was not available, the etching was done using RIE. The parameters used for reactive ion etching are as follows. The pressure was set to 60mTorr at power 100W. The gases used in reactive ion etching were SF₆ at 25 sccm and O₂ at 5 sccm. The process was ran for 30 minutes. After etching, the depth was measured using ZETA 3D optical profiler. Both square spiral channel and circular spiral channels were etched. After measurement, it was found that the average depth was found to be 15 μ m. Further etching was not possible with the machine, so for this work, we decided not to use dry etching and use wet etching.

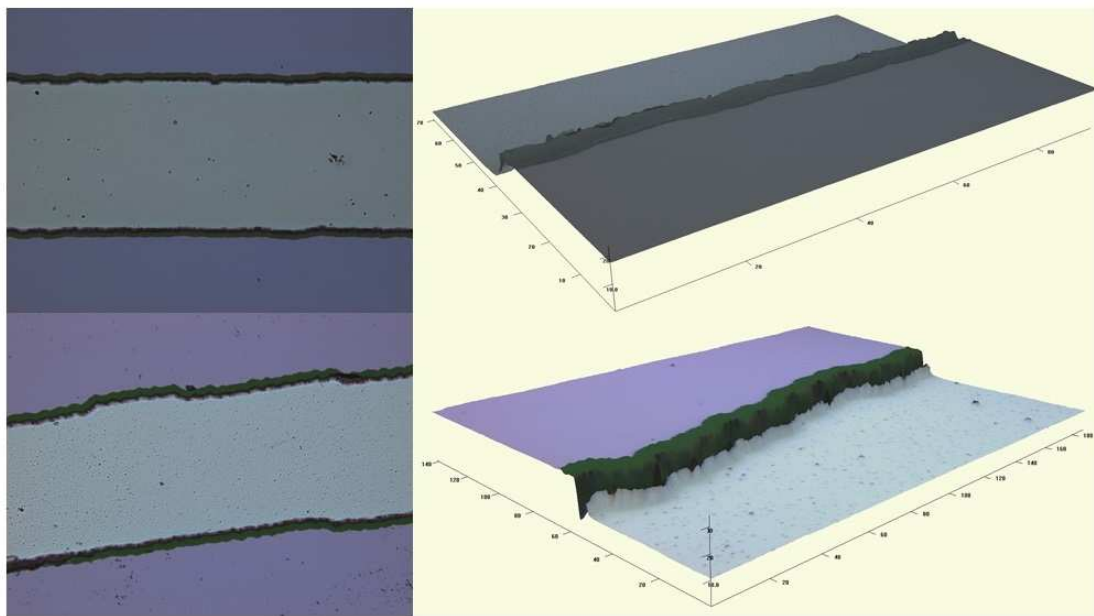


Figure 3.10: 2D and 3D images taken using profilometer after RIE for square (top) and circular (bottom) spiral channels

After these experiments, it was decided to use square spiral channels etched in 25 wt% TMAH solution at 90 °C as explained in section 3.2.2.

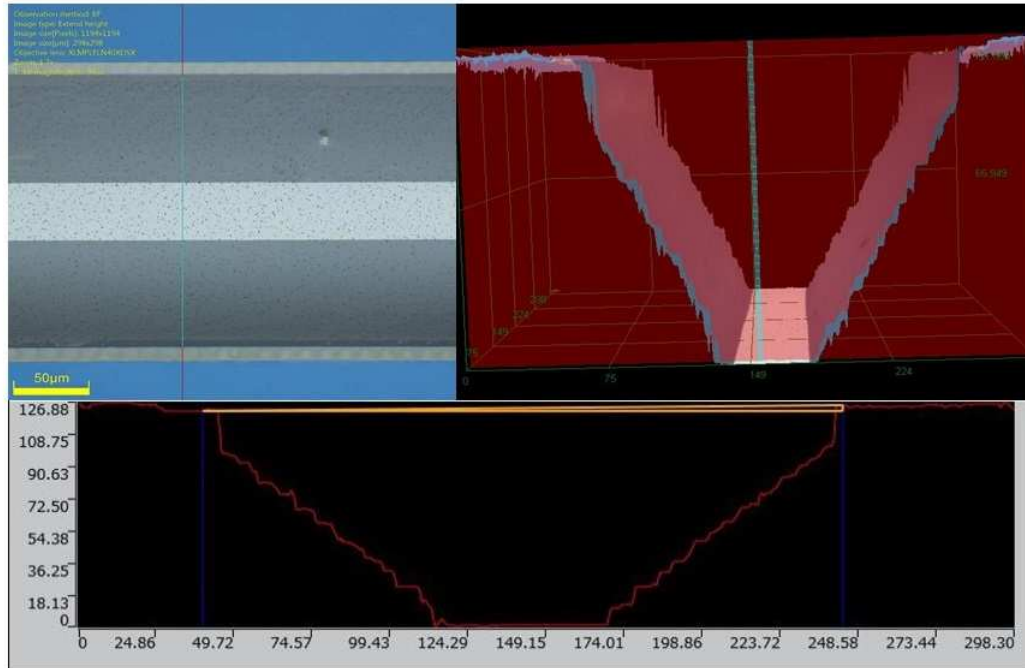


Figure 3.11: 2D (top left), 3D (top right) and histogram (bottom) showing the depth of the square spiral channels etched in TMAH for 3 hours

3.3 Bonding

When fabrication of the channels are done, the sealing of the channels were done using PYREX glass. For bonding, silicide bonding was chosen. Inlet and outlet holes were drilled on the PYREX glass wafer. PYREX glass was drilled with 2 mm drill bits using glass drilling machine. Once the inlet and outlet holes were drilled, the glass wafer was cleaned with piranha solution at 90 °C for 10 minutes. The wafer was then rinsed with DI water and dried. Next step was to coat the intermediate metallic layer on to the wafer. For this process, electron beam evaporator was used. Ti was chosen as the metallic layer.

Evaporation is a physical vapour deposition technique where the target material is heated to melt it and the vaporized metal particles move towards the substrate. This PVD technique takes place under vacuum, typically 10^{-5} or even lesser. A high voltage in the range of kV is sent through a tungsten filament, which heats the filament to the thermionic emission point. At this point, thermionic emission of electrons takes place from tungsten. This filament is located outside the deposition zone. This arrangement is done to avoid contamination of the deposited layer. The electrons emitted from the filament are focussed and directed towards the crucible where the target material. The metal to be deposited is the target. This focussing and directing is done by means of electromagnets. When the electron beam hits the target, the kinetic energy of the electrons are transferred to heat through the impact of hitting the target. This transfer of energy by several millions of electrons will generate very high heat energy which is capable of melting the target metal. By focussing the electrons localized heating of the target is possible which can elevate the temperature to very high levels ranging several hundreds of degrees. High levels of vacuum is created

for avoiding contamination.

Electron beam evaporator uses electron beam for melting the target metal. Electron beam will be concentrated to the target and this causes melting of the target. For evaporator, the maximum power was set to be 42 percentage. Titanium pellets which acts as the target was filled in silica crucible and the electron beam was adjusted to fall into the crucible. The thickness was set to 92 nm. The evaporator had automatic thickness controller and the deposition will stop once the thickness reaches the preset value. The temperature at the target will be 40-45 °C. The evaporation process initiated when the chamber pressure reached below 5×10^{-5} . This helped to avoid any possible contamination during deposition process. The vaccum level was achieved by two steps, with the help of a rotary pump and a cryo pump. The rotary pump creates a vaccum to the level of 10^{-2} and after that cryo was turned on which will pick up from that pressure level to further below. Cryo cannot be used directly to create high vaccum levels from atmospheric pressure level.

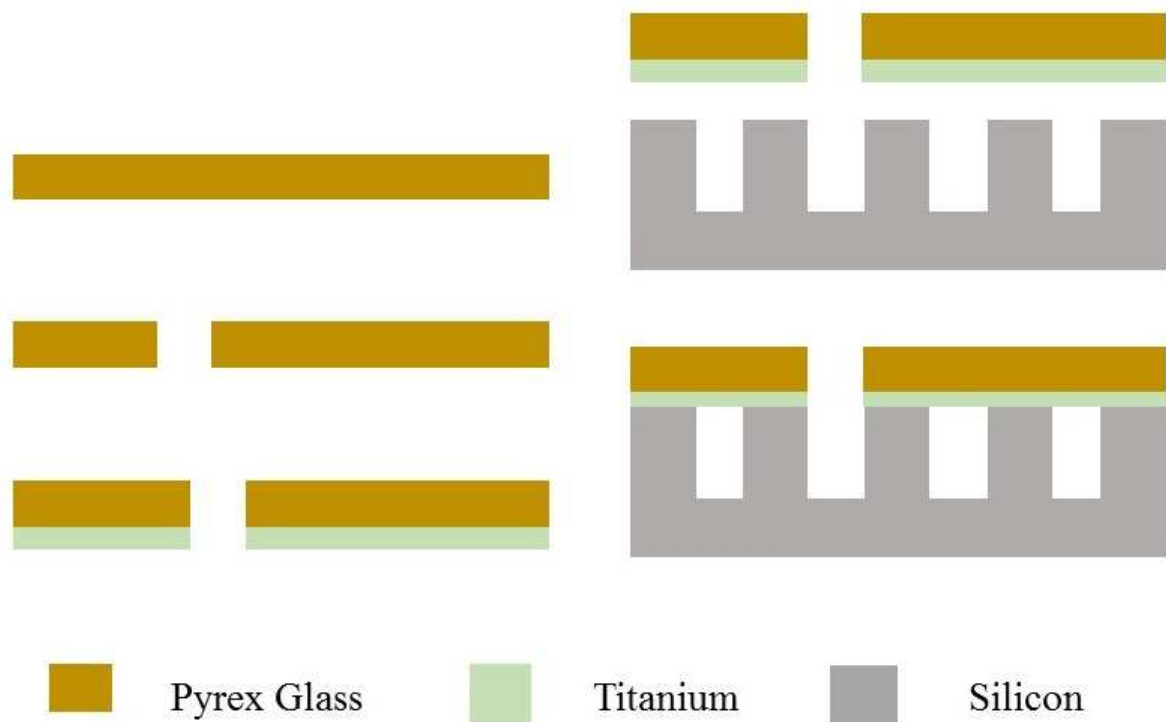


Figure 3.12: Process flow for bonding of microfabricated channel and pyrex glass

After deposition of the intermediate metal layer, the PYREX glass substrate was demounted from the evaporation chamber. As titanium is a slow oxidising material, the chances of fast oxidation is less. But to avoid the contamination of the surface, the coated substrate was kept in vaccum as soon as possible. The clean room facilities available were not high standards. So the metal deposited wafer was kept in vaccum within very less time. The silicon wafer which has the channels fabricated on it was also cleaned and kept into vaccum within no time. After etching the channels in TMAH, the oxide which acted as the mask was not removed immediately. The oxide etching was done just before the bonding process. The oxide was removed by dipping the wafer in BHF and

then thoroughly rinsed with DI water. Special care has to be taken to ensure that both the samples to be bonded are extremely clean and the presence of every minute particle will cause voids in the bonding interface.

Silicide bonding was done on AML wafer bonder. The wafers were placed into the bonding chamber. The chamber was purged with nitrogen. Bonding was done by applying high pressure and temperature. The bonding force was set to 1kN and temperature was 377 °C. The force was applied slowly and temperature was increased in steps. The temperature was increased in steps of 50 °C. The force and temperature was kept at above values for 45 minutes. The bonding process flow is shown in Fig. 3.12.

The bonded wafers were analysed for bonding quality. Sonoscan was done for this bond quality analysis. Sonoscan used ultrasonic sound for analysing the bonding interface. An ultrasonic source is placed over the analyte, i.e., the bonded sample. The sample is immersed in water. The sample is fixed in a stage which is immersed in water. The ultrasonic source is placed on a movable stage, which also houses the sensor to capture the reflections. The bonded parts of the sample will reflect the ultrasonic waves and those parts which are not bonded will not pass waves through those portions. So the bonded parts appear as black and portions that are not bonded appear as white in the image.

Chapter 4

Appendix

4.1 Acoustic separation of particles

Microfluidics is the science and technology of designing and developing systems or devices that can process very small amount of fluids typically in microlitres to femtolitres. For this micrometer sized channels are used. For a microfluidic channel, at least one dimension of the channels should be in micrometer scale (ie, tens or hundreds of micrometers). Fluids in these micro sized channels behaves differently than they do normally. Microfluidic devices exploit these physical and chemical properties of fluids in microscale. Microfluidics when combined with MEMS fabrication technology can create devices used for precise analysis and processing of fluids. Microfluidic devices which uses very less amount of fluids in analysis makes it applicable to many fields especially medical and biological applications. The application of microfluidics devices also includes and not limited to cell biology, glucose tests, chemical microreactor, electrochemistry, microprocessor cooling etc.

When MEMS actuators and sensors are considered, two most important principles that are utilized for detection and sensing are, electrostatics and piezoelectricity. Piezoelectricity has been used as a mode for actuation in many MEMS devices. The piezoelectric materials are materials those can convert the electrical excitation provided to mechanical force and viceversa. Piezoelectricity and piezoelectric materials are extensively explored for mEMS actuators and sensors. These piezoelectricity based sensors are used as pressure sensors, energy harvestors, torque sensors etc.

Particle separation devices are one of the most widely explored and interesting devices among researchers. Separation of particles are very necessary in purification compounds as well as detection of specific component in a mixture. Particle separators are also useful in biomedical field also where several detection processes can be done. Separation of particle is also needed in environmental analysis and detection of different particles in air, complex mixtures such as petroleum products etc. Specific detection devices use many techniques such as chemical assay, chemiresistive methods, colorimetric methods, capacitance based, resistance based etc. Particle separation devices was of high interest from older days itself. So many techniques such as filtration, distillation etc were used from olden days itself.

Nanosized and microsized particle separation is of very high interest today. These have applications in nanotechnology applications such as cancer diagnosis and treatment, targeted drug delivery.

sensing and detection, photonics etc. There has been several techniques used for the separation of nanoparticles. Electrophoresis, dielectrophoresis, magnetic separation methods etc are very few of the techniques used for nano and micro sized particle separation.

Suspended particles in fluid are affected by the acoustic forces when they are introduced into an acoustic wave field. Acoustic waves generate pressure gradients across the field. These pressure gradient and the acoustic forces can be used to manipulate suspended particles and fluid medium. Since acoustic forces are non contact forces, these manipulations won't cause any harm or mutation to any of the particles in the fluid stream. When compared to the electrical, optical and magnetic methods of manipulation, these acoustic manipulations are perfect in particle manipulation processes. As there will be no effect of mutations to the particle, this method is very well suitable for biological applications and can be integrated to a LAB on chip device. This method is non invasive, the particles do not need any kind of pretreatment, no need of markers and labels etc. Recent studies have shown the effectiveness of using acoustic separation methods for manipulation of cells and particles.

4.2 Background

Recently, acoustic based separation techniques have drawn significant attention as it is cost effective, label free, non contact. Acoustic based separation techniques are used for particle separation in continuous flow [14]. Piezoelectricity is the basic principle used here. When an alternating electric potential is applied to a piezoelectric material, a mechanical pressure is generated in the material. This mechanical pressure will be in the form of deformations on the surface of the material. When there are two different electric fields applied, the deformations on the surface will constructively interfere to form surface waves. These surface waves will interact with any fluid domain in the vicinity of the piezoelectric material surface. The fluid will absorb energy from the surface waves as they pass along the surface. The absorbed energy will be in the form of longitudinal pressure waves that propagate through the fluid. These surface acoustic waves interact with different particles in the fluid and causes manipulation of the particles in the fluid. This principle is used for separation of micro and nano sized particles.

Piezoelectric materials when excited with external electric field will generate Bulk acoustic waves and Surface acoustic waves. Previously both BAW and SAW were used in particle manipulation [15]. But BAW are not well suitable for this application because of the materials that are used for making the microchannels for fluid flow over the piezoelectric material surface. Polydimethylsiloxane is the most extensively used and widely accepted material for fabrication of microchannels. Generation of the bulk acoustic waves require rigid microchannel walls with extremely good reflection properties. But PDMS has very poor acoustic reflection properties. Also for a lab on chip application, it is difficult to integrate a bulk transducer to the system. So, BAW is not a good option for acoustic based lab on chip devices.

Interdigitated devices are used for SAW generation. Recently, researchers have shown the use of SAW for focussing, separating, aligning, directing and manipulating fluid in microchannels [16]. SAW are actually sound waves that propagate through the surface of an elastic material. Most of the energy of the SAW is confined to one or two wavelength depth of the substrate surface. SAW can

be generated with any frequency upto GHz.

4.3 Device structure and Principles

Surface acoustic waves include Rayleigh wave, sheath horizontal surface acoustic waves, surface skimming bulk waves, leaky surface waves and many others. SAW generally travel along the surface at one or two wavelength depth from the surface. SAW are generated by applying sinusoidal electric potential to inter digitated electrodes. IDTs are finger like structures that were firstly reported for SAW generation in 1665 [ref saw]. IDTs are formed with two comb like metal structures whose fingers are located periodically in alternating pattern. When potential is applied, because of inverse piezoelectric effect of the substrate on which the IDTs are fabricated, a stress variation is generated on the surface. When there are two set of IDTs placed in opposite directions, there will be two set of fields generated and they constructively interfere to form a standing surface acoustic wave. SSAW generates a pressure nodes (maximum pressure points) and anti-pressure nodes (minimum pressure points) periodically in the fluid domain in touch with the piezoelectric substrate. The position of these are controllable and can be used for manipulation of the particles in the fluid domain [14].

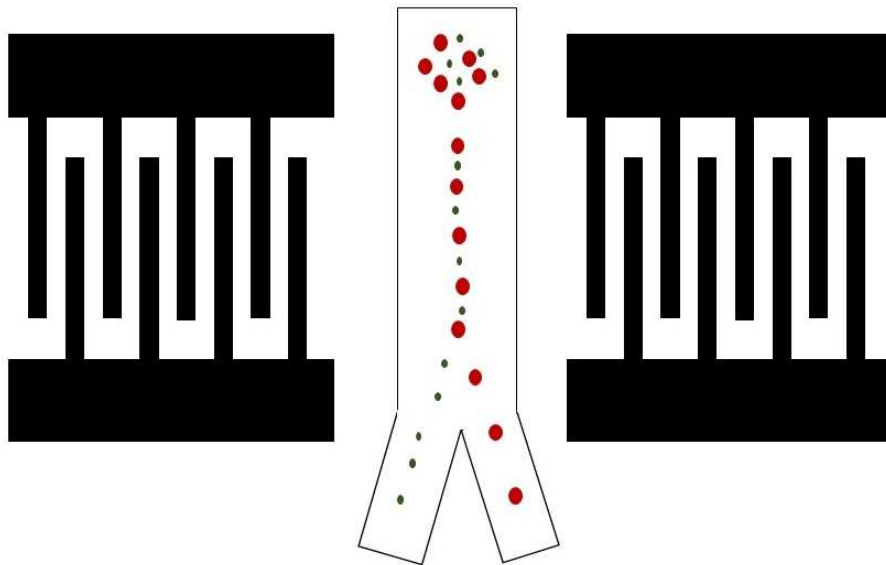


Figure 4.1: Schematic of the SSAW based device showing separation and focussing

Figure 4.1 shows the schematic of a SSAW device . The device consists of a piezoelectric substarte, IDTs and a channel. The channel is generally fabricated by PDMS. The IDTs can be fabricated on the sustrate using metal deposition and patterning. Once the electrodes are fabricated on the substrate, the channel which has already been fabricated is bonded to the substrate. The channel is formed on PDMS with the help of soft lithography techniques. The mould of the channel

is formed on a silicon wafer and photoresist, normally SU8, by patterning with appropriate mask using lithography technique. PDMS mixed with adequate amount of curing agent is poured on to the mould and allowed to solidify by heating at a particular temperature. This makes the pattern on PDMS. This fabricated structure is then carefully removed from the mould. The channel is then plasma bonded to the substrate surface in between the IDTs. Figure 4.2 shows the SSAW propagating along the surface of the piezoelectric substrate and the channel.

The particles flowing through the channel along with the fluid will be influenced by several forces such as the acoustic radiation, viscous drag, hydrodynamic forces and diffusion forces. Among these, gravity force is almost equal in magnitude to buoyancy forces and opposite in direction to those. So buoyancy forces will get cancelled with the gravity forces.

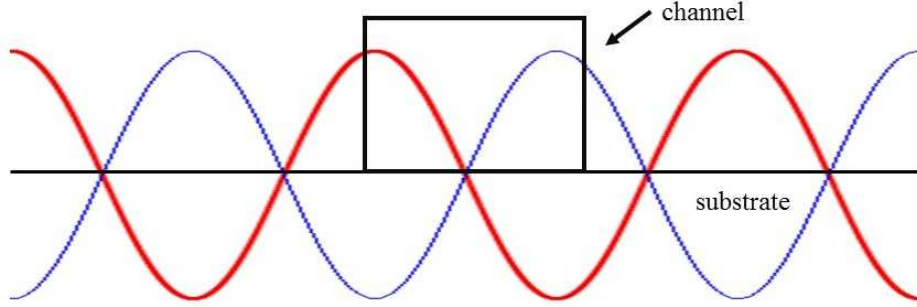


Figure 4.2: Schematic of the SSAW propagating along the surface of the piezoelectric substrate and extends to the channel

The behaviour of the particles in the channel can be understood by analysing the drag force and the acoustic radiation force. Acoustic radiation force depend on th volume of the particle, whereas, the drag force depends on the radius of the particle. The drag force (F_d) is represented by Eq. 4.1 and acoustic radiation force is represented by Eq. 4.2.

$$F_d = -6\pi\mu R_p u_r \quad (4.1)$$

$$F_r = \frac{-(\pi p_0^2 V_p \beta_w)}{2\lambda} \phi(\beta, \rho) \sin(2ky) \quad (4.2)$$

$$\phi = \frac{5\rho_p - 2\rho_m}{2\rho_p + \rho_m} - \frac{\beta_p}{\beta_m} \quad (4.3)$$

where p_0 is the acoustic pressure, V_p is the volume of the particle, ρ_p is the density of the particle, ρ_m is the density of the medium β_p is the compressibility of the particle, β_w is the compressibility of the medium, λ is the acoustic wavelength, μ is the viscosity of the medium, u_r is the relative velocity of the particle and k is the wavenumber of the standing acoustic wave. From Eq. 4.2 it is understood that the radiation force acting on a particle is a function of volume of the particle, density of the particle, compressibility of the particle and the power applied to IDTs. So, particles with differences in these properties will experience variation in acoustic radiation force.

In Eq. 4.3, ϕ is the acoustic contrast factor, which determines whether the particle will move to a pressure node or an anti-pressure node. The particle will aggregate at pressure nodes when ϕ is positive and will aggregate to anti-pressure node when ϕ is negative. Most of the particles and cells in aqueous solution have positive ϕ and move towards pressure node.

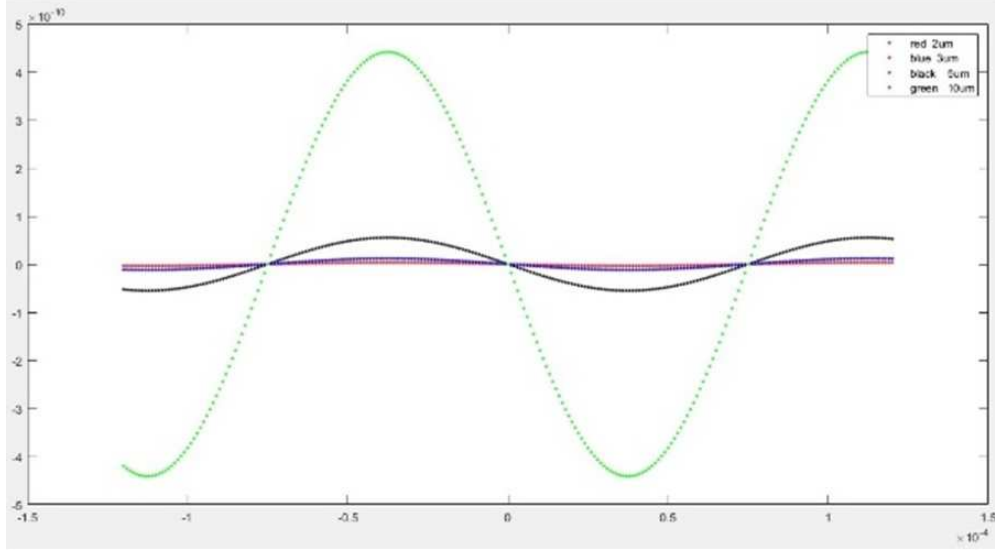


Figure 4.3: Acoustic radiation force along the channel on different particle sizes

The acoustic force pushes the particles to move from anti-pressure nodes to pressure nodes in the SSAW field. The time taken to reach the pressure node depends on the acoustic radiation force amplitude on the particle. The magnitude of acoustic force depends on the size of particle and compressibility. Larger particles will have high magnitude of acoustic radiation force acting on it which results in higher lateral displacement within lesser time. Smaller particles will take more time to move the same distance. This difference in time taken to reach the same point by different sized particles is responsible for the separation of particles. By changing the flow velocity, channel length and the SAW power, the particles can be separated and the separation performance can be improved. By adjusting the position of the nodes and anti nodes, the distribution of particle also changes. Figure 4.5 shows this change.

4.3.1 Effect of tilted angle SSAW

The separation efficiency can be improved by introducing a tilted angle SSAW [17]. Ding et al [17] introduced a unique configuration of tilted-angle standing surface acoustic waves (taSSAW), which are oriented at an optimally designed inclination to the flow direction in the microfluidic channel. They introduced the concept of tilt in the channel as shown in Fig. 4.4. The pressure nodes and anti pressure nodes will be tilted wrt flow direction. The effect of this tilt can be included in the acoustic radiation force and drag force by introducing an angle dependency in the equation.

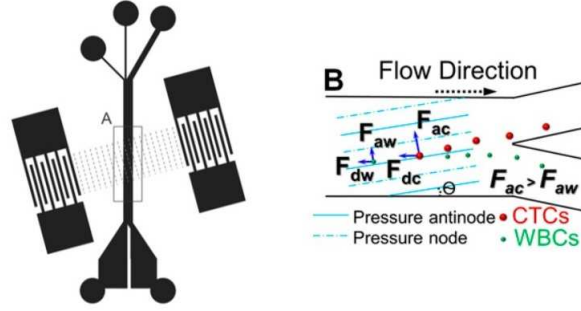


Figure 4.4: Schematic diagram of the tilted SSAW separator showing the pressure and antipressure nodes as dashed lines [17]

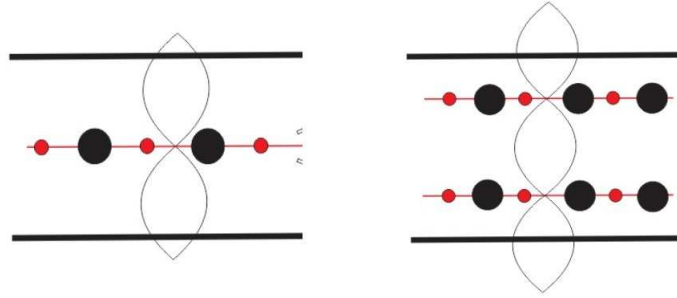


Figure 4.5: orientation of particles with different sizes according to the orientation of pressure nodes and antipressure nodes

$$\frac{dx}{dt} = u_f \cos \theta \quad (4.4)$$

$$\frac{dy}{dt} = u_f \sin \theta + u_r \quad (4.5)$$

where u_f is the fluid velocity in an infinitely long channel with a rectangular cross section, u_r is the velocity of the particle due to the acoustic radiation force imposed by the standing surface acoustic wave, and t is time.

$$u_f = \frac{\delta P b^2}{2\mu} \left[1 - \frac{Z^2}{b^2} + 4\Sigma \frac{(-1)^n \cosh(\alpha_n \frac{Y}{b}) \cos(\alpha_n \frac{z}{b})}{\cosh(\alpha_n \frac{a}{b})} \right] \quad (4.6)$$

$$u_r = \frac{\pi R_p^2 p_0^2 \beta_w}{9\lambda\mu} \phi(\beta, \rho) \sin(2ky) \quad (4.7)$$

$$\alpha_n = (n - \frac{1}{2})\pi \quad (4.8)$$

where δP is the pressure gradient, X, Y, Z are coordinates in the flow direction and x, y, z are coordinated in the tilted axis.

4.4 Simulation and Results

The numerical simulation of acoustic separation device was done using COMSOL multiphysics 5.2. Comsol allows to couple different physics and analyse the overall effect of multiple interactions on the device. 128° Y cut LiNbO_3 was used as the piezoelectric material. IDTs were fabricated on the substrate with aluminium. The microfluidic channel was madeup of PDMS. Water was used as the fluid medium passing through the channel. There will be five physics interactions taking place in the device.

For modelling the piezoelectricity, solid mechanics(solid) module and electrostatics(es) modules were coupled. Electrostatics module was used to apply electric potential to the IDTs. 10 vpp was the applied potential. This applied potential across the IDTs will drive the SAW field across the channel. Solid mechanics module was used for modeling the piezoelectric domain and the elastic domains. All the domains except the fluidic channel were given as solid. The LiNbO_3 domain was given as piezoelectric material. Bottom surface of the substrate was given as fixed boundary to avoid any possible deformations on that side.

An impedance analysis was conducted to find the practical resonant frequency of the device. For that electric displacement was simulated in frequency domain analysis and the displacement was plotted against frequency. The total displacement plotted against frequency is shown in Fig. 4.6. It is showing resonant frequency of 9.4 MHz which is same as the calculated value.

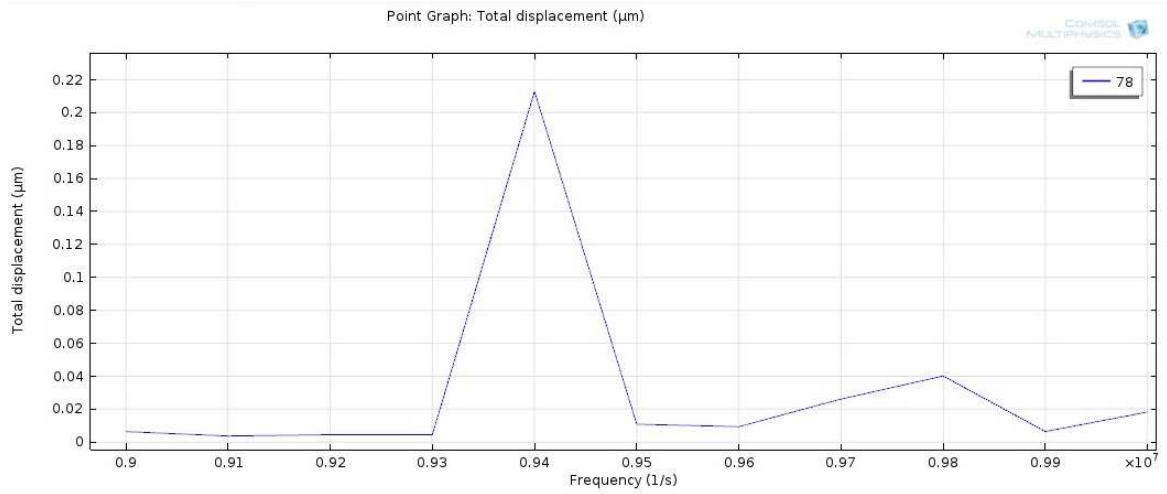


Figure 4.6: Total displacement plotted against frequency for finding resonant frequency

For modeling the acoustics physics, pressure acoustics, frequency domain (acpr) was used. Pressure acoustics module can be coupled with the solid mechanics and electrostatics module in frequency domain for acoustic analysis. This coupled multiphysics will consider the piezoelectric effect and take the effect to create the acoustics field. Pressure acoustics was given only to the fluid domain. The walls of the channel was given as plane wave radiation boundaries.

The pressure acoustics was simulated in frequency domain to find the acoustic pressure field generated in the fluid domain. When a sinusoidal potential is applied to the IDTs the surface

deformation on the piezoelectric substrate makes pressure vibrations in the fluid domain. This was simulated as total acoustic pressure in frequency domain analysis at the resonant frequency obtained from the displacement simulation. This gives the standing surface acoustic waves generated in the fluid domain. The pressure variation can be analysed through this simulation. Figure 4.7 shows the acoustic pressure field generated in the channel region by the SSAW.

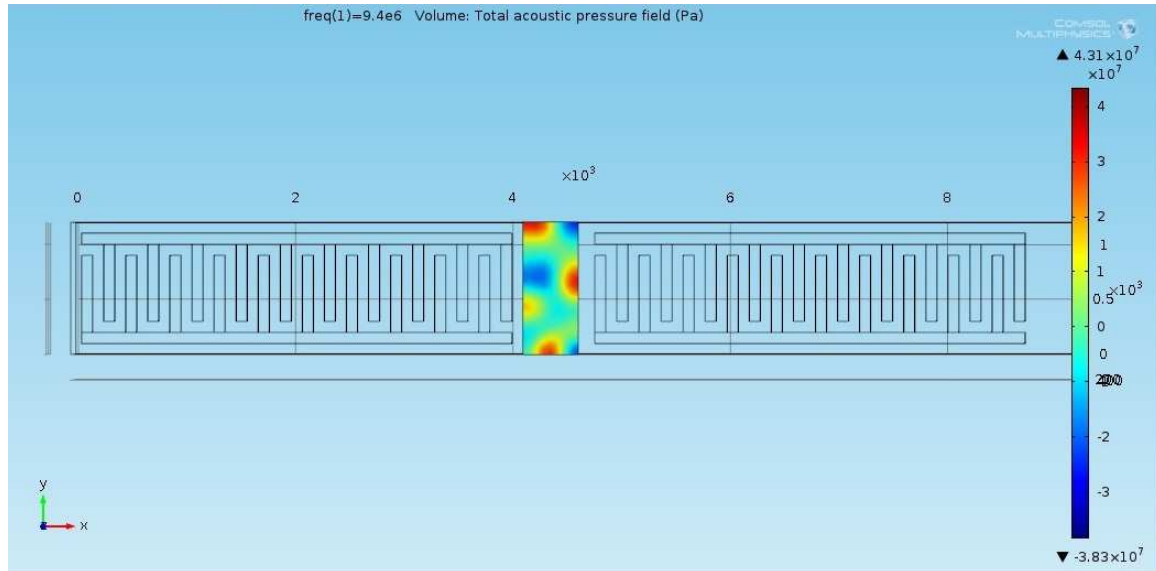


Figure 4.7: Acoustic pressure field generated in the channel region by the SSAW

The distribution of pressure nodes and anti-pressure nodes were also studied. By changing the position of the microchannel in between the IDTs, the pressure and anti-pressure nodes can be placed according to the design for either focussing or separation of the particles. Figure 4.8 shows the distribution of the pressure nodes when the IDTs are placed at different distance from the channel. If there is one pressure and antipressure node along the surface of the channels, then the channel will focuss the particles to the central line between the nodes. If there is more than one pressure and anti-pressure nodes, the particles will get separated according to the size.

The orientation of the pressure node nad anti-pressure node can be placed according to the distance of the channel from the IDTs. Figure 4.9 shows the orientation in which the channel was placed at 100 and 200 μm from the IDTs from left an dright respectively

After simulating the acoustic pressure field, a flow simulation was done to know the seperation of particles due to the SSAW wave generated acoustic field. For the flow simulation, laminar flow (sp) physics was used. This defines the inlet and outlet of the channel and the flow velocity of the fluid flowing through the channel. Laminar flow physics generates the laminar flow velocity and a damping force due to the flowing fluid.

A particle tracing physics has to be applied in order to simulate the particle flow through the channel. For that particle tracing module (fpt) was added to the model. Particle tracing module

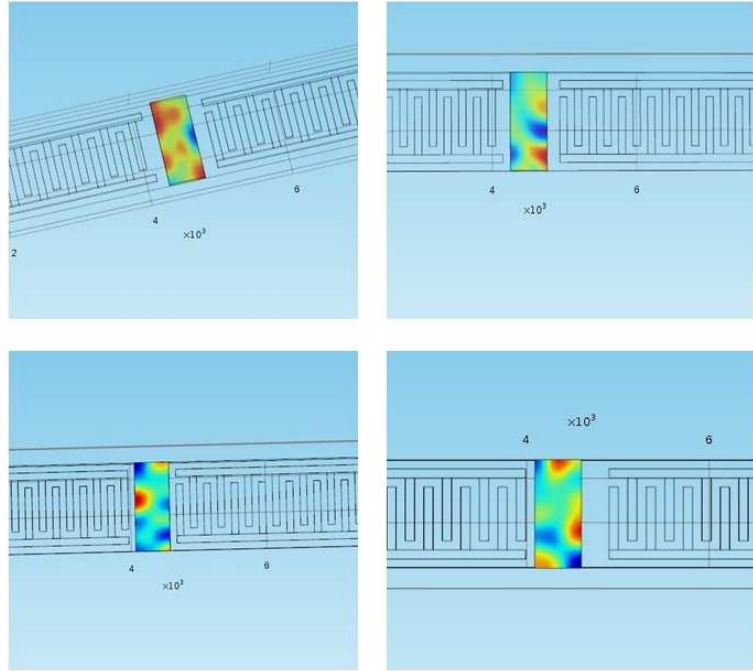


Figure 4.8: Distribution of the pressure nodes when the IDTs are placed at different distance from the channel

enables to define different particle properties flowing through the channel along with the fluid defined in the laminar flow module. This also enables to define different forces acting on the particles while passing through the channel. Damping force due to the laminar flow and viscosity of the fluid and acoustophoretic force due to the acoustic field are the two forces acting on particles in this simulation. The simulation was first done to focus the particles to the centre of the channel. So the channel was placed in between the channels according to the previous simulations. Figure 4.10 shows the acoustic pressure field and Fig. 4.11 shows the particle trajectory through the channel. It is shown that the particles will focus to the centre of the channel. The particle with higher diameter will move to the centre faster when compared to particle with lower diameter as shown in Fig. 4.11.

4.4.1 Effect of tilted angle

After simulation of the pressure acoustics and particle flow, the effect of the tilt angle explained as in section 4.2.2 was analysed. As explained in principles the tilt with respect to IDTs introduced in the channel can affect the separation. Figure 4.13 shows the effect of the tilted channel on particles with different diameters. It is observed that particle with higher diameter displaces more when compared to particle with lower diameter. The separation takes place according to the difference in this vertical displacement.

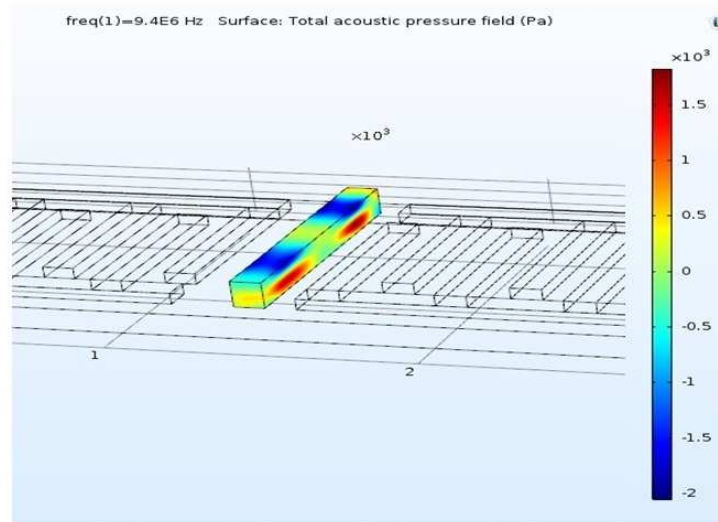


Figure 4.9: Distribution of the pressure nodes when the IDTs are placed at a distance from the channel such that anti pressure nodes come in centre and pressure node comes at sides of the channel

The effect of tilt angle was also studied. The displacement of a particle with $10 \mu\text{m}$ diameter, density 1.05 kg/m^3 , flow rate $9 \mu\text{L/min}$, compressibility 2.16×10^{-10} at awavelength of $300 \mu\text{m}$ was simulated at two tilt angles, 10° and 30° . Figure 4.14 shows the result of this simulation. It was observed thta displacemnt is more for 30° when compared to 10° .

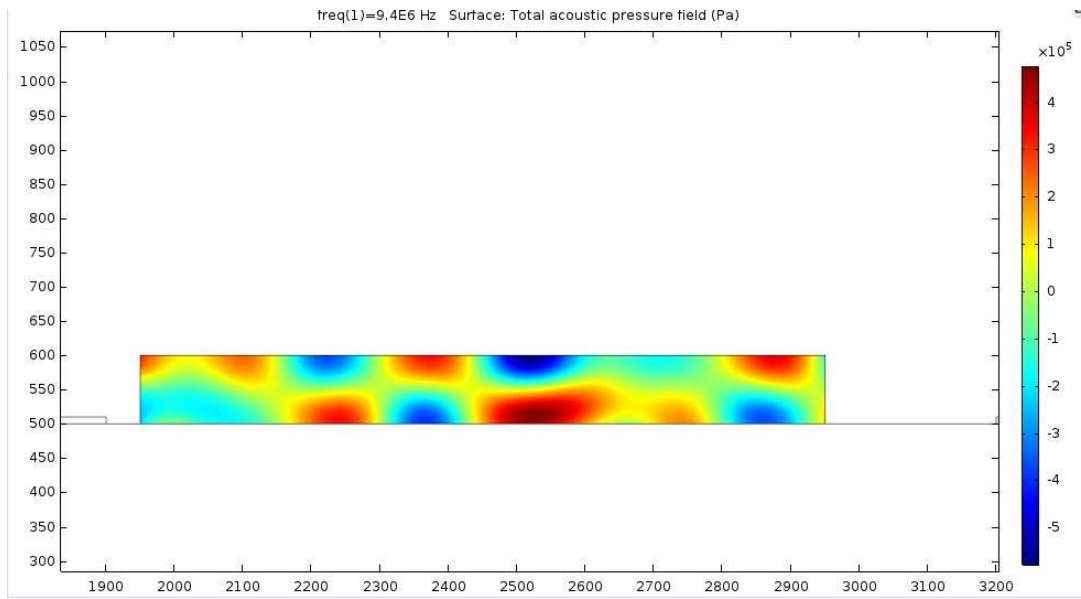


Figure 4.10: Distribution of the pressure nodes when the IDTs are placed at a distance from the channel such that anti pressure nodes and anti pressure nodes will come at the sides of the channel and the channel will focus the particles

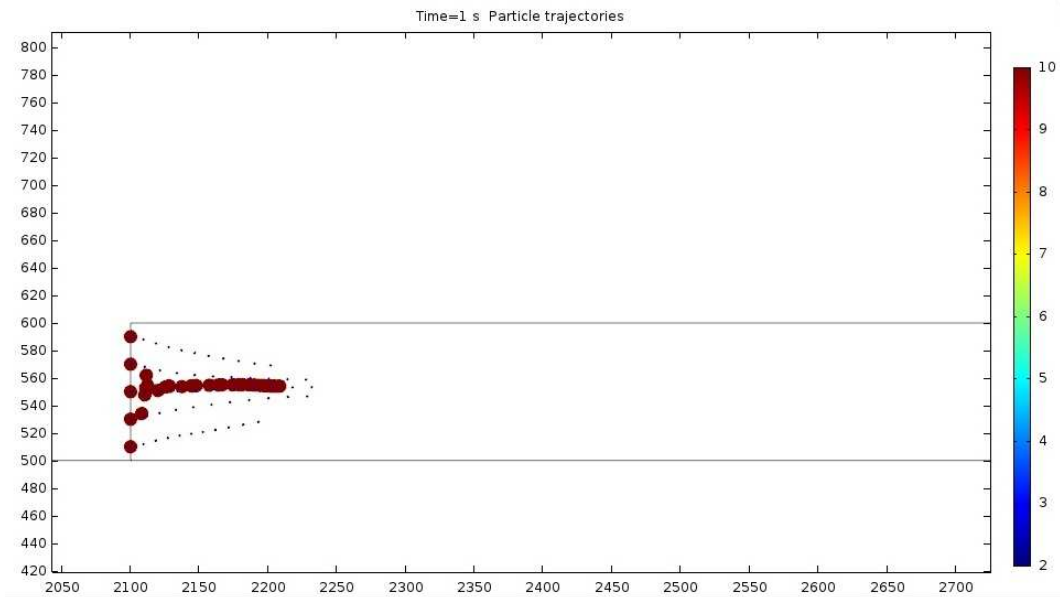


Figure 4.11: The trajectory of two particles with different diameters when introduced to a channel which focusses the particles.

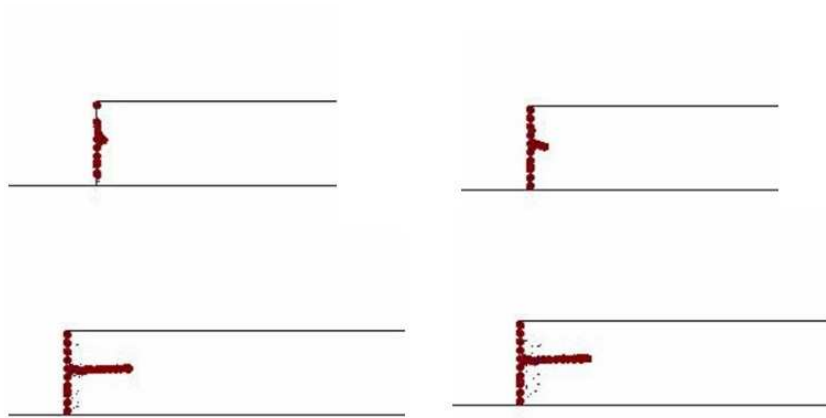


Figure 4.12: The trajectory of two particles with different diameters when introduced to a channel which focusses the particles at different time instances at a time step of 0.1s .

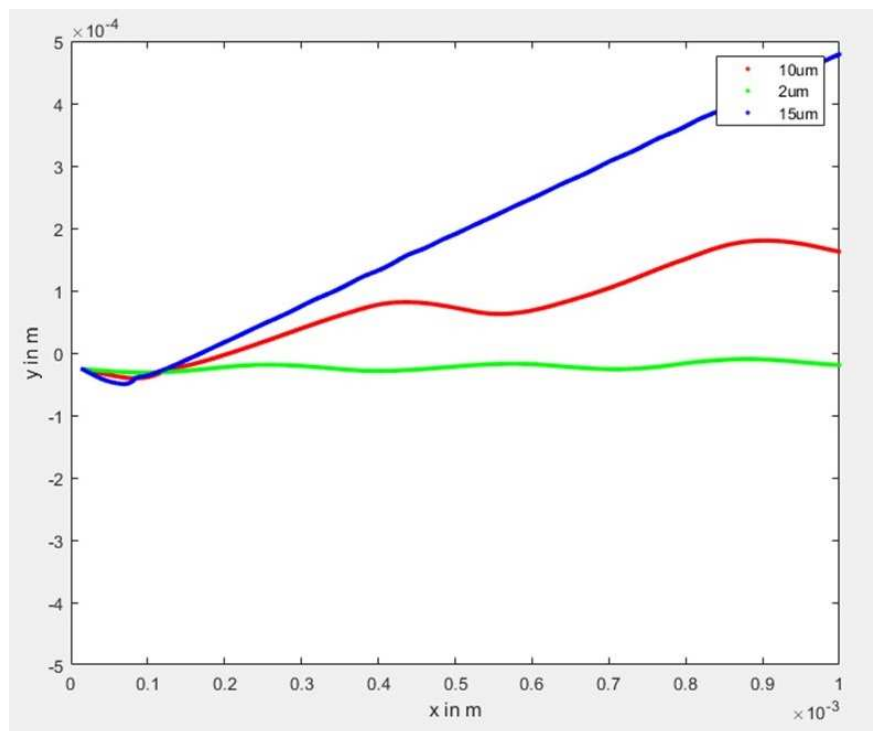


Figure 4.13: The displacement of the particle with different diameters as the effect of the tilted channel

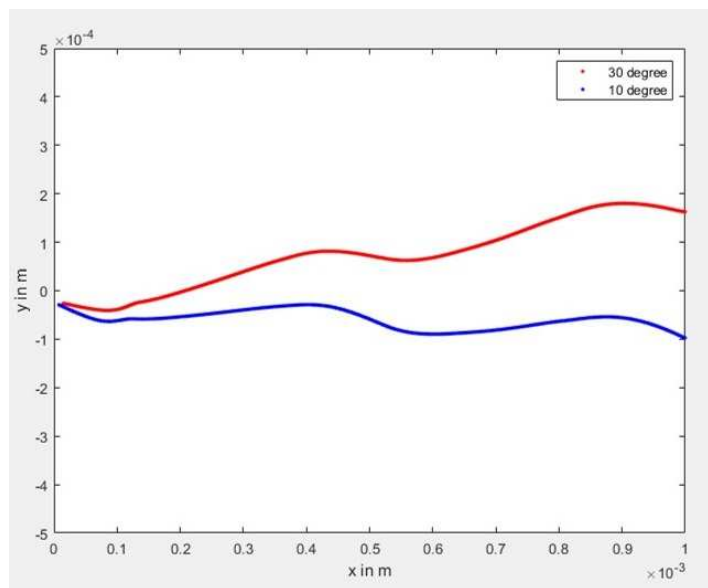


Figure 4.14: The displacement of the particle with same diameter at different angles

References

- [1] Grob L Robert and Barry F Eugene. Modern Practice of Gas Chromatography, Fourth Edition. 2004.
- [2] M. Akbar, M. Restaino, and M. Agah. Chip-scale gas chromatography: From injection through detection. 2015.
- [3] G. Serrano, T. Sukaew, and E. T. Zellers. Hybrid preconcentrator/focuser module for determinations of explosive marker compounds with a micro-scale gas chromatograph. *Journal of Chromatography A* 1279, (2013) 76 – 85.
- [4] M. Navaei, P. Hesketh, J. Xu, A. Mahdavifar, J. M. Dimandja, and G. McMurray. All Silicon Gas Chromatographic Column for Fast Separation of VOCs Released By *Armillaria Fungus*. *Meeting Abstracts* MA2015-01, (2015) 2094.
- [5] S. C. Terry, J. H. Herman, and J. B. Angell. A Gas Chromatographic Air Analyzer Fabricated on a Silicon Wafer. 1979.
- [6] C. J. Lu, W. H. Steinecker, W. C. Tian, M. C. Oborny, J. M. Nichols, M. Agah, J. A. Potkay, H. K. Chan, J. Driscoll, R. D. Sacks, K. D. Wise, S. W. Pang, and E. T. Zellers. First-generation hybrid MEMS gas chromatograph. 2005.
- [7] G. Lambertus, A. Elstro, K. Sensenig, J. Potkay, M. Agah, S. Scheuering, K. Wise, F. Dorman, and R. Sacks. Design, Fabrication, and Evaluation of Microfabricated Columns for Gas Chromatography. 2004.
- [8] M. Agah, G. R. Lambertus, R. Sacks, and K. Wise. High-speed MEMS-based gas chromatography. 2006.
- [9] Y. Li, X. Du, Y. Wang, H. Tai, D. Qiu, Q. Lin, and Y. Jiang. Improvement of column efficiency in MEMS-Based gas chromatography column. 2014.
- [10] A. Garg, M. Akbar, S. Narayanan, L. Nazhandali, and M. Agah. Zebra GC: A fully integrated micro gas chromatography system. 2014.
- [11] A. D. Radadia, A. Salehi-Khojin, R. I. Masel, and M. A. Shannon. The fabrication of all-silicon micro gas chromatography columns using gold diffusion eutectic bonding. 2010.
- [12] Y. Jiang, G. Liu, and J. Zhou. A novel process for circle-like 3D microstructures by two-step wet etching. 2009.

- [13] M. Yao, B. Tang, K. Sato, and W. Su. Silicon anisotropic etching in Triton-mixed and isopropyl alcohol-mixed tetramethyl ammonium hydroxide solution. *IET Micro Nano Letters* 10, (2015) 469–471.
- [14] J. Shi, H. Huang, Z. Stratton, Y. Huang, and T. J. Huang. Continuous particle separation in a microfluidic channel via standing surface acoustic waves (SSAW). *Lab on a Chip* .
- [15] M. Wu, Z. Mao, K. Chen, H. Bachman, Y. Chen, J. Rufo, L. Ren, P. Li, L. Wang, and T. J. Huang. Acoustic Separation of Nanoparticles in Continuous Flow. *Advanced Functional Materials* .
- [16] M. Haddadi, B.; Fathipour. Numerical analysis of 3D model of the SSAW separator system. *Int. J. Comput. Appl.* 712.
- [17] X. Ding, Z. Peng, S.-C. S. Lin, M. Geri, S. Li, P. Li, Y. Chen, M. Dao, S. Suresh, and T. J. Huang. Cell separation using tilted-angle standing surface acoustic waves. *Proceedings of the National Academy of Sciences* .